The influence of exercise during weight loss on muscle remodeling during colon cancer induction in mice

Sophia Roubos
B.Sc., Queen's University 2016

THESIS

Submitted to the
Faculty of Graduate and Postdoctoral Studies
In partial fulfillment of the requirements
For the degree of Master's of Science – Human Kinetics

Faculty of Health Science, School of Human Kinetics
University of Ottawa, Canada

© Sophia Roubos, Ottawa, Canada, 2018

CONTENTS

Part I

Literature Review

Introduction

Colorectal cancer (CRC) is the second most commonly diagnosed cancer in males and third in females (Canadian Cancer Statistics, 2017). CRC is also linked to several modifiable risk factors, such as obesity (Canadian Cancer Statistics, 2017). Obesity increases an individuals risk of developing CRC by approximately 30% (Ma et al., 2013). As such, individuals living with obesity are often recommended to lose weight through diet and exercise to reduce their CRC risk (American Cancer Society, 2018). However, weight loss by diet and exercise can also alter skeletal muscle remodeling. Skeletal muscle remodeling is the change in composition of muscles following damaging stimuli and can involve alterations in many pathways including protein synthesis, degradation, and regeneration (Potthoff, Olson, & Bassel-Duby, 2007). Alterations in skeletal muscle remodeling are important in people with CRC because approximately 50% of these individuals also develop cachexia, a multifactorial syndrome characterized by a progressive loss of skeletal muscle mass (Argilés, Busquets, Stemmler, & López-Soriano, 2014; Kumar et al., 2010). This loss of skeletal muscle mass is associated with increased morbidity, mortality, and a reduction in both tolerance to cancer treatment and quality of life, implicating a vital role of skeletal muscle in this condition (Donohoe, Ryan, & Reynolds, 2011). Currently, there are no therapeutic options for patients with cachexia, thus prevention and identifying early contributors to cachexia could improve outcomes in patients with CRC (Kumar et al., 2010). Along these lines, it is important to understand how weight loss and exercise, two lifestyle modifications recommended to individuals at increased risk of developing CRC, influence muscle remodeling during CRC initiation. Currently, this information is lacking in the literature. Therefore, the

purpose of this study was to determine the effects of obesity followed by weight loss with or without exercise on skeletal muscle remodeling during CRC induction.

Muscle-resident stem/progenitor cells in muscle remodeling

Skeletal muscle is a relatively stable, post-mitotic tissue, yet still possesses the unique ability to undergo regeneration (Collins & Partridge, 2005). Critical to this process are satellite cells, myogenic stem cells located between the basal lamina and the sarcolemma (Mauro, 1961). The expression of various myogenic regulatory factors regulates the progression and commitment of satellite cells to the myogenic lineage. All satellite cells express Pax7 (Seale et al., 2000). In healthy, unstressed muscle, satellite cells are quiescent (Snow, 1977). In response to injury; however, satellite cell activation, proliferation ($Pax7^{+}MyoD^{+}$), and differentiation ($Pax7^{-}MyoD^{+}$) occurs to repair muscle fibers (Davis, Weintraub, & Lassar, 1987; Seale et al., 2000; Yin, Price, & Rudnicki, 2013). The down regulation of Pax7 towards the end of differentiation allows myoblasts to exit the cell cycle so they can form new skeletal muscle fibers or fuse to existing fibers (Olguin, Yang, Tapscott, & Olwin, 2007). The importance of satellite cells to the regenerative process has been confirmed by studies where ablating satellite cells led to a loss of regeneration in skeletal muscle (Lepper, Partridge, & Fan, 2011; Murphy, Lawson, Mathew, Hutcheson, & Kardon, 2011; Sambasivan et al., 2011).

Satellite cells are also part of a dynamic, complex microenvironment that dictates their progression through myogenesis. Key cellular components of the satellite cell niche are fibro/adipogenic progenitors (FAPs). FAPs are a population of non-myogenic skeletal muscle-resident progenitors, distinct from satellite cells, that reside interstitially between muscle fibers (Yin et al., 2013). FAPs can be identified by their expression of $PDGFR\alpha^{+}$ (A Uezumi et al., 2014). Communication between satellite cells and FAPs is essential for effective satellite cell mediated

regeneration and maintenance of the muscle microenvironment (Joe et al., 2010). FAPs are bipotent, and have the potential to differentiate into adipocytes and fibrocytes resulting in the deposition of fatty and fibrotic tissue, respectively (Joe et al., 2010). In response to injury in healthy regenerating muscle, FAPs proliferate before satellite cells and support the myogenic program by providing a transient source of pro-differentiation signals (Boppart, De Lisio, Zou, & Huntsman, 2013; Hu et al., 2010; Joe et al., 2010). Without FAPs communicating with satellite cells, myogenesis is impaired (Roberts et al., 2013).

In the following sections, the effects of cachexia, obesity and exercise on muscle remodeling during CRC progression will be explored. This review will focus specifically on how cachexia, obesity and exercise influence satellite cells, and FAPs on muscle remodeling during CRC progression, due to their importance to the regeneration of muscles.

The influence of cachexia, obesity and exercise on muscle remodeling

Cachexia develops in approximately 50% of CRC patients after diagnosis, while obesity increases an individuals risk of developing CRC (Kumar et al., 2010; Ma et al., 2013). Weight loss is recommended to reduce risk of CRC, but this may exacerbate cachexia, which is characterized by decreased caloric intake. Exercise may be a viable strategy to maintain muscle mass during weight loss in patients with CRC to prevent cachexia. There are no studies that examine the effects of obesity, followed by weight loss, with or without exercise on muscle remodeling during CRC progression.

Cachexia and muscle remodeling

As CRC progresses, there is the potential for some patients to develop cachexia, a multifactorial syndrome characterized by a progressive loss of skeletal muscle (Argilés et al.,

2014). In human cancer patients with and without cachexia, a reduction in cross-sectional area (CSA) in type I and type IIA fiber types has been observed (Toth et al., 2016). Factors released from the tumor induce a systemic inflammatory response that create a chronic state of degeneration in skeletal muscle (Talbert & Guttridge, 2016). This induces a regenerative response in skeletal muscle to maintain muscle mass (Talbert & Guttridge, 2016). Recent evidence suggests that impaired satellite cell function and the subsequent reduced regenerative potential contribute to cachexia (Hu et al., 2010). Muscles isolated from both preclinical models and biopsies from pancreatic cancer patients have shown clear indications of myofibre structural damage due to circulating factors (He et al., 2013; Mehl, Davis, Berger, & Carson, 2005; Talbert, Metzger, He, & Guttridge, 2014). Associated with these indicators of fibre damage, there has also been an increase in activated satellite cells, large increases in Pax7 expression, but no increase in transcription factors that are markers of differentiation (He et al., 2013; Penna et al., 2011; Sciorati et al., 2009; Talbert et al., 2014). It appears, then, that the myogenic program is dysregulated in cancer cachexia and fibers are in a constant state of regeneration with impaired differentiation (Mehl et al., 2005). The exact mechanism through which this aberrant Pax7 signalling occurs has yet to be elucidated; however, the current literature suggests two possible reasons (Talbert & Guttridge, 2016). Downstream, there is evidence to suggest that the increased levels of Pax7 inhibit the expression of MyoD and myogenin, impeding the ability of myoblasts to fuse to damaged fibers (He et al., 2013). Upstream, it has been reported that the activation of NF-κB in cachectic muscles induces dysregulation of Pax7 and subsequent loss of muscle, as the deletion of NF-κB signalling was sufficient to rescue the muscle loss associated with cancer cachexia (He et al., 2013). *In vitro* and *in vivo* studies have found that the inhibition of regeneration in cachetic mice is reversible when the tumor is removed, which is important from a therapeutic perspective (He et

al., 2013). Myoblasts isolated from tumor bearing mice then cultured in differentiation medium were still able to differentiate once removed from the tumor environment (He et al., 2013). This finding was corroborated *in vivo*, as when C-26 tumors (a model of CRC) were surgically removed, there was a 3-fold increase in myoblast fusion and significant increase in muscle fiber size (He et al., 2013). Therefore, these results suggest that the impaired regeneration observed in cachexia is a reversible process (He et al., 2013). Thus, it is clear that cancer cachexia represents a pathological condition that can damage muscle fibers and initiate the regenerative process, without the successful repair of muscle fibers, ultimately inducing muscle loss (Talbert & Guttridge, 2016). It remains unknown; however, how patient characteristics known to influence muscle mass, such as weight status and participation in exercise interventions, influence myogenic stem cell function during CRC initiation.

Few studies have examined the role of FAPs in cancer cachexia. Ablation of fibroblasts, a cell population that overlaps with FAPs, exacerbated cachexia (Roberts et al., 2013). He et al. (2013), discovered that non-satellite cell progenitors, identified by their expression of $Sca1^+$ and $CD34^+$, expand after myofiber damage in mice with cancer cachexia. Some of these cells co-expressed $PDGFR\alpha^+$, a marker of FAPs, suggesting an involvement of FAPs in cancer cachexia, though their role in this condition was not determined (He et al., 2013). Findings from Roberts et al. (2013) indicate that in mice bearing the C-26 colon carcinoma, FAPs are decreased and this is associated with an alteration in their ability to produce ECM components (Roberts et al., 2013). Considering that the composition of the ECM is necessary for proper functioning of myogenesis, the authors speculate that the tumor environment may result in FAPs altering the composition of the extracellular matrix (ECM), thereby altering myogenesis, which would contribute to the

muscle loss observed in cancer cachexia (Roberts et al., 2013). Together, it appears that FAPs are dysfunctional in cancer cachexia; however, future studies are necessary to determine their role.

Obesity and muscle remodeling

Obesity is also a condition characterized by impaired muscle regeneration (Akhmedov & Berdeaux, 2013). As such, it may potentiate muscle loss during CRC progression. In murine models of diet-induced obesity, impaired muscle regeneration has been observed (Fu et al., 2016; Tatsumi, Hattori, Ikeuchi, Anderson, & Allen, 2002). Although, the mechanisms underlying this process are poorly understood. The current literature suggests that regeneration is impaired in individuals with obesity due to reduced satellite cell function. Following freeze injury in young mice fed a high fat diet (HFD), satellite cell content was decreased and impaired regeneration was observed in the tibialis anterior (TA) muscle (Woo et al., 2011). Furthermore, mice receiving a HFD for 8 months displayed decreased TA muscle mass, smaller myofibers and increased collagen deposition relative to lean mice after cardiotoxin injury (Hu et al., 2010). Potential mechanisms implicated in the reduced regenerative capacity of muscle from HFD-fed mice are decreased MyoD and impaired satellite cell activation (D'Souza et al., 2015; Tatsumi et al., 2002). Pincu and colleagues (2015) found that a concomitant HFD and exercise protocol did not result in any changes in mean myofibre CSA, but did increase the number of fibres between 500-1000 μm^2 in size (Pincu, Linden, Zou, Baynard, & Boppart, 2015). The signals causing this satellite-cell mediated impaired regeneration in obesity are currently unknown.

With obesity, there is also an increase in fatty and fibrotic tissue in skeletal muscle (Akhmedov & Berdeaux, 2013). More specifically, increased fatty acids produced because of obesity accrue in muscle as intramyocellular lipids (IMCLs) and as intermuscular adipose tissue (IMAT), with IMCLs being found primarily in lipid droplets containing perilipins (Kalinkovich &

Livshits, 2017). *In vivo,* it has been shown that when FAPs are transplanted into healthy muscle, there is no evidence of FAP engraftment or donor-derived adipocytes (Joe et al., 2010). Yet, when FAPs are transplanted into muscles characterized by fatty infiltration, FAPs differentiated into adipocytes (Joe et al., 2010). Thus, it appears that rather than releasing trophic factors that favour myogenic differentiation and regeneration, FAPs may be contributing to fibrotic and fatty tissue infiltration in obesity. Treadmill training during high fat feeding did not alter muscle mesenchymal stromal cell (mMSC) content, a population that overlaps with FAPs (Pincu et al., 2016). The mechanisms determining the fate of FAPs and their role in regeneration in obese models are unknown.

Collectively, it appears that obesity is a condition that may impair muscle remodeling by decreasing satellite cell content and increasing the amount of fibrotic and fatty tissue accumulation from FAPs.

Exercise and muscle remodeling

A cancer diagnosis is also often accompanied by reduced physical activity, which suggests that there is ample opportunity for exercise-based interventions (Courneya & Friedenreich, 1997; Irwin et al., 2003). Exercise may be a way of mitigating the effects of cachexia on muscle, by influencing the dysregulated pathways. For example, in a mouse model of colon cancer, treadmill running was able to prevent the progression of cachexia (Gould, Lahart, Carmichael, Koutedakis, & Metsios, 2013). This may be due to reduced inflammation (Bowen, Schuler, & Adams, 2015).

Exercise has the potential to mitigate muscle wasting through stimulating muscle-resident stem/progenitor cells to contribute to improving muscle remodeling. Exercise is a physiological stimulus that damages muscle and activates satellite cells, which then proliferate and differentiate

to repair muscle fibers (Bossola, Marzetti, Rosa, & Pacelli, 2016). Recently, Farup et al. (2015) found that prolonged resistance training was able to increase satellite cell and FAP content within muscle (Farup et al., 2015). Furthermore, transplanting FAPs into pre-exercised limbs elucidated their indirect contribution to satellite cell expansion and new fiber synthesis, suggesting that exercise positively regulates FAP function (Huntsman et al., 2012; Valero, Huntsman, Liu, Zou, & Boppart, 2012). Zou et al. (2015) found that when FAPs were transplanted in adult mice following repeated bouts of eccentric exercise, myofiber size increased, and there was increased myonuclei (Zou et al., 2015). The mechanism through which this occurs has yet to be elucidated. Huntsman et al. (2012) found that FAPs release anti-inflammatory cytokines after removal from exercised muscle, demonstrating that perhaps exercise is a non-pharmacological cue that dictates the function of FAPs (Huntsman et al., 2012). No studies have examined the effects of exercise specifically on satellite cell and FAP function relative to muscle remodeling during CRC progression.

Statement of the problem and rationale

Obesity and exercise are two modifiable risk factors associated with CRC. As such, weight loss, either through diet and/or exercise, is recommended in people at risk of developing CRC. There is evidence to suggest that obesity followed by weight loss alone may exacerbate muscle loss due to the caloric deficit, while exercise may help maintain muscle mass during weight loss. It remains unknown; however, if a combined diet and exercise strategy is superior to diet alone at maintaining muscle mass, and muscle-resident stem/progenitor cell populations during CRC progression. Therefore, the current thesis seeks to determine whether exercise during diet-induced weight loss can mitigate muscle atrophy and maintain muscle stem/progenitor cell populations during CRC progression in an azoxymethane (AOM) mouse model. An understanding of how

these factors may alter muscle remodeling may provide valuable information involving early indicators of muscle loss that may be augmented by weight loss and may provide cellular targets for future treatments.

Aims and Hypothesis

The objectives of this study are to determine the combined effect of weight loss, with or without exercise, on muscle mass and stem/progenitor cells populations during CRC induction in an AOM mouse model.

We hypothesize that exercise will increase muscle mass and indicators of stem/progenitor cell-mediated muscle remodeling after weight loss during CRC progression in an AOM mouse model.

Significance

Approximately 50% of patients with CRC experience skeletal muscle loss associated with cachexia and currently there is no treatment (Argilés et al., 2014). Skeletal muscle loss is an important prognostic indicator, independent of total body weight loss (Martin et al., 2013). There is evidence to suggest that exercise may maintain muscle mass during weight loss induced by caloric deficit. However, the effects of weight loss with or without exercise on muscle maintenance during CRC progression have not been studied. Therefore, results of this thesis will further our understanding of how the myogenic program is regulated under a combination of weight loss, exercise, and cancerous conditions. This is significant because it is expected to highlight the need for the addition of exercise interventions for maintaining muscle mass during weight loss in CRC. As such, future studies can aim at determining whether this response will be similar in humans. Furthermore, elucidating the function of muscle resident stem/progenitors in this process will aid

in a better understanding of the cellular mechanisms involved in this process and potentially identify novel cellular targets for therapeutic interventions. Lastly, studying the progression of CRC will allow for the identification of early indicators of cachexia that may be exacerbated by weight loss. Thus, if we can identify factors that are early indicators of cachexia that may be worsened by weight loss, this may allow for early intervention in patient populations who are at increased risk of cachexia.

PART II

Article

The influence of exercise during weight loss on muscle remodeling during colon cancer induction in mice

Sophia Roubos[1], Donna D'Souza[1], Russell Emmons[2], Diego Hernandez-Saavedra[3], Guanying Xu[3], Yuan-Xiang Pan[3], Hong Chen[3], and Michael De Lisio[1]

[1]School of Human Kinetics, University of Ottawa, Ottawa, ON. [2]Departments of Kinesiology and Community Health, and [3]Food Science and Human Nutrition, University of Illinois at Urbana-Champaign, Urbana, IL.

Running head: Weight loss, exercise, and cachexia

Key words: Satellite cells, fibroadipogenic progenitors, cachexia, fibrosis, adiposity

Corresponding author information:

Dr. Michael De Lisio

University of Ottawa,

School of Human Kinetics,

200 Lees Avenue, Room E260E

Lees Campus

K1N 6N5

(613) 562-5800 (6987)

Email: mdelisio@uottawa.ca

ABSTRACT

Background: Diet and exercise have been recommended to reduce the risk of colorectal cancer (CRC) in individuals with obesity. However, the effects of these interventions on muscle remodeling during CRC initiation in individuals who were previously obese is unknown. Since CRC is associated with a high-risk of cachexia, it is important to understand how diet and exercise interventions can impact muscle remodeling in populations at risk of developing CRC-induced cachexia. Our aim was to investigate the effects of weight loss, with or without exercise, on markers of muscle remodeling in a mouse model of CRC. We hypothesized that exercise plus weight loss would increase muscle mass, reduce muscle fibro/fatty tissue, and increase muscle stem/progenitor cell content compared to weight loss alone.

Methods: Mice consumed a high-fat diet (HFD) to induce obesity or a control (CON) diet. Subsequently, mice received injections of azoxymethane (AOM) to induce CRC. Then, weight loss was induced in HFD mice by placing them on the CON diet and those mice either remained sedentary (HFD-SED) or completed a treadmill exercise intervention (HFD-EX).

Results: After 40 weeks, mice were sacrificed and analyzed for markers of muscle remodeling. HFD-SED and HFD-EX showed weight loss and a loss in percent fat mass when looking at changes between sacrifice and before AOM injections ($p<0.05$ vs. CON). HFD-SED and HFD-EX had increased lean mass ($p<0.05$ vs. CON), and HFD-EX had increased tibialis anterior (TA) weight ($p<0.05$ vs. CON). The proportion of medium-sized fibers increased ($p<0.05$ vs. HFD-SED and CON) in HFD-EX, but there were no differences in overall cross-sectional area, myonuclei per fiber, or myonuclear domain. HFD-SED had increased fibrosis ($p<0.05$ vs. HFD-EX and CON) and adiposity ($p<0.05$ vs. CON). The number of committed ($Pax7^{+}MyoD^{+}$) satellite cells (SCs) and FAPs was greater in HFD-EX ($p<0.05$ vs. CON). There were no differences in uncommitted

(Pax7^{+}MyoD^{-}) or differentiated (Pax7^{-}MyoD^{+}) SCs. Additionally, nuclear p-NF-κB was reduced following exercise ($p<0.05$), specifically in the interstitium with a significant decrease in the number of interstitial p-NF-κB cells in the HFD-EX group ($p<0.05$ vs. CON and HFD-SED).

Conclusions: Findings suggest that a HFD, followed by weight loss with exercise, can reduce fibrotic and fatty degeneration of the muscle and improve markers of muscle remodeling. These findings provide the rationale to further examine exercise interventions for maintaining muscle quality during weight loss interventions to reduce CRC-induced cachexia.

INTRODUCTION

In Canada, colorectal cancer (CRC) is the second most frequently diagnosed cancer in males and third in females[1]. Non-hereditary lifestyle factors can influence an individuals' risk of developing CRC[1]. Obesity is one such factor and can increase the risk of developing CRC by approximately 30%[2]. Considering this, individuals with obesity are often recommended to lose weight through diet and exercise to reduce their CRC risk[3]. Since weight loss is the result of a reduction in both muscle and adipose tissue[4], it may exacerbate CRC-associated cachexia. Approximately 50% of CRC patients develop cachexia, a loss of skeletal muscle mass, which is associated with increased morbidity, mortality, and a reduction in both tolerance to cancer treatment and quality of life[5,6]. Despite this knowledge, there are no studies that look at the effects of obesity followed by weight loss, with or without exercise, on skeletal muscle remodeling during CRC induction for potential early indicators of cachexia.

It is widely accepted that skeletal muscle remodeling is regulated by the coordination of two muscle-resident stem/progenitor cell populations: satellite cells and fibroadipogenic progenitors (FAPs). Satellite cells are the skeletal muscle resident myogenic stem cells that are typically quiescent ($Pax7^{+}MyoD^{-}$)[7]. In response to injury, they are activated, become committed ($Pax7^{+}MyoD^{+}$) and differentiate ($Pax7^{-}MyoD^{+}$) to form new myofibers or fuse to existing fibers through a process known as myogenesis[8–10]. FAPs proliferate prior to satellite cells after injury and provide a transient source of pro-myogenic factors that facilitate satellite cell differentiation[11]. Depletion of these cell populations severely impairs muscle remodeling[12–15]. Understanding how lifestyle modifications influence progenitor cell populations in skeletal muscle could identify early indicators of cachexia, a condition for which there is currently no therapy.

The current literature suggests that both cachexia and obesity are associated with impaired muscle remodeling[16,17]. Indeed, muscles from both pre-clinical models and biopsies from pancreatic cancer patients have shown increases in Pax7 expression but no increase in transcription factors that are markers of differentiation, suggesting impaired myogenic commitment is a key contributor to cachexia[18–21]. Little is known about the role of FAPs with respect to cancer cachexia. Muscles from cachetic patients and pre-clinical models, however, are characterized by muscle atrophy and fibro/fatty tissue accumulation[18,22]. In one previous study, deleting fibroblasts, a cell population that overlaps with FAPs, exacerbated cachexia in a mouse model of cancer cachexia, suggesting they play a key role in maintaining muscle health during wasting[15]. Under cachetic conditions, the NF-κB pathway has been found to upregulate Pax7 expression and prevent differentiation of satellite cells[18]. Furthermore, Hyldahl et al. (2013) found that NF-κB activity is localized to the interstitium and acts in a cell-autonomous manner to inhibit myoblast differentiation[23]. Comparatively, in models of obesity, satellite cell content has been found to be decreased[24]. Regarding FAPs, when FAPs are transplanted into muscles characterized by fatty infiltration, rather than releasing trophic factors to facilitate myogenesis, they differentiate into adipocytes[11], suggesting they may promote the fibro/fatty tissue accumulation in muscle in obesogenic conditions. With obesity, increases in TNF-α have been linked to muscle loss[25]. Considering this, it is possible that obesity followed by weight loss alone may exacerbate muscle loss, especially during the initiation of CRC, through dysregulation of muscle-resident progenitors.

Exercise has been found to facilitate the myogenic program and maintain muscle mass under healthy conditions. Recently, Farup et al. (2015) found that prolonged resistance training was able to increase satellite cell and FAP content within muscle[26]. Furthermore, transplanting FAPs into pre-exercised limbs elucidated their indirect contribution to satellite cell expansion and

new fiber synthesis, suggesting that exercise positively regulates FAP function following acute exercise, likely via paracrine mechanisms[27,28]. Endurance exercise has also been found to reduce fibrosis and inflammation in skeletal muscle in mice with obesity[29]. In mouse models of cancer cachexia, treadmill running has been found to increase muscle mass and strength[21,30]. The effects of exercise may be mediated by stimulated myoblast differentiation as Penna and colleagues (2011) reported a reduction in the Pax7 accumulation that is typically observed in mouse models of cachexia[21]. Treadmill training during high fat feeding did not alter FAP, termed muscle-derived mesenchymal stem cells, content[31]. It remains unknown; however, if a combined weight loss and exercise strategy is superior to weight loss alone at maintaining muscle mass, and muscle-resident stem/progenitor cell populations during CRC initiation.

As such, the purpose of this study was to determine the combined effect of weight loss, with or without exercise, on muscle health and stem/progenitor cell populations during CRC induction in an azoxymethane (AOM) mouse model. We hypothesize that exercise will increase muscle mass and indicators of stem/progenitor cell-mediated muscle remodeling after weight loss during CRC progression in an AOM mouse model compared to weight loss alone.

METHODS

Study Design

Ethical approval was obtained from the Illinois Institutional Animal Care and Use Committee. This study represents analysis of muscle tissue derived from mice whose bone marrow and CRC induction data has been submitted in a separate manuscript (Emmons, unpublished). A total of 36 male C57BI6/J (Jackson Laboratories) mice were maintained in a 12:12 hour light-dark schedule with food and water provided *ad libitum*. At 5 weeks of age, mice were randomly divided into control (n=12; CON) or high fat diet (n=24; HFD) groups. The control diet consisted of 10%

kcal fat (AIN-93M, Research Diets). Comparatively, mice fed the HFD received a diet consisting of 45% kcal fat for 8 weeks (D12451, Research Diets) to induce obesity. At 13 weeks of age, those mice on the HFD returned to the control diet. All mice also received weekly intra-peritoneal injections of AOM for 4 weeks beginning at 13 weeks of age. During the first week, mice received a dose of 15 mg/kg of AOM (MRI#600, MRIglobal). During the subsequent 3 weeks, 10 mg/kg of AOM (MRI#600, MRIglobal) was administered each week. Mice were weighed weekly throughout the study and lean mass was collected using EchoMRI-100 (Echo Medical Systems) based upon previous protocols[32].

Progressive exercise training program

From 0 to 23 weeks of age, all mice were sedentary. At week 23, those mice that were on a HFD, then switched to the CON diet at 13 weeks of age, were divided into an exercise (n=12, HFD-EX) and sedentary (n=12, HFD-SED) group. The mice in the exercise group were exercised on a motorized treadmill (Columbus instruments) for 22 weeks (i.e. from week 23 to 45), 3 days per week. Each training session consisted of: (1) A 10-minute warm up at a speed of 12 m/min, (2) A training period that progressively increased in duration and speed, and (3) A 5-minute cool down at a speed of 12 m/min.

At the beginning of the exercise intervention, mice exercised during the training period at 10 m/min for 25 minutes. The duration increased by 10 minutes per week, until a 45-minute training time was reached. Once a 45-minute training duration was reached, speed was increased every week by 1 m/min (starting at week 25) until a speed of 23 m/min was reached, at which point the mice continued to exercise at this pace until week 45. Electric shock was not used as encouragement. To ensure all mice were under similar stress throughout the study, CON and HFD-SED mice were also placed on treadmills for 1 hour, 3 times per week.

Euthanasia and tissue collection

At 45 weeks of age, mice were sacrificed by CO_2 asphyxiation followed by cervical dislocation. Tibialis anterior (TA) muscles were collected and frozen in precooled isopentane. The TA was cut at the midline, down the axial plane and embedded in optimum cutting temperature (Tissue-Tek; Fischer Scientific). Using a cryostat (Leica, Wezlar, Germany), transverse cryosections (8 µm nonserial sections) were cut to conduct histological assessments. These sections were then placed on frozen microscope slides (Superfrost; Fischer Scientific, Hanover Park, IL) and stored at -80^{o}C.

Immunohistochemistry

Slides were thawed and washed in 1XPBS. Subsequently, they were fixed in 2% paraformaldehyde for 10 minutes at room temperature, followed by washes in 1XPBS and permeabilization of the membrane with 0.1% triton x-100 for 10 minutes at room temperature. Then, sections were washed in 1XPBS and blocked with either: mouse on mouse (MOM) Ig blocking reagent (Pax7 and dystrophin) for 1 hour at room temperature followed by the MOM diluent (Pax7 and dystrophin) for 5 minutes at room temperature, or 5% GS, 1% BSA and 0.1% triton x-100 (p-NF-κB and perilipin) for 1 hour at room temperature. After, primary antibodies were applied overnight at 4^{o}C (Pax7, dystrophin, p-NF-κB and perilipin) followed by a series of washes in 1XPBS. Subsequently, sections were incubated in their appropriate secondary antibodies. Next, sections were washed in 1XPBS and re-blocked in 5% GS, 1%BSA and 0.1% triton x-100 (MyoD, laminin) or DAKO (PDGFRα) for 1 hour at room temperature. Then, primary antibodies were applied overnight at 4^{o}C (PDGFRα and laminin). A primary cocktail consisting of MyoD and laminin was also applied overnight at 4^{o}C. Thereafter, the appropriate secondary antibodies were applied for 1 hour at room temperature, followed by washes in 1XPBS. Then,

nuclei were stained with DAPI (1:10 000) for 5 minutes and washed again in 1XPBS. Lastly, paramount was applied and sections were cover slipped. Samples were stained against the following primary antibodies: Pax7 (neat, Developmental Studies Hybridoma Bank, University of Iowa, Iowa City, USA), MyoD (1:100, Abcam, Cambridge, U.K.), laminin (1:200, ThermoFisher Scientific, Massachusetts, USA), PDGFRα (1:500, R&D Systems, Minnesota, USA), p-NF-κB (1:200, Cell Signaling Technology, Massachusetts, USA), perilipin (1:100, Cell Signaling Technology, Massachusetts, USA) and dystrophin (1:200, Sigma Aldrich, St. Louis, Missouri, USA). Following the primary antibodies, the appropriate secondary antibodies were applied at 1:300 (Pax7, Laminin, PDGFRα, perilipin) or 1:200 (MyoD, dystrophin, p-NF-κB). Antibodies were confirmed using secondary only controls. Sections were also stained following Masson's Trichrome protocol[33].

Immunohistochemistry quantification

All images were captured using the EVOS FL Auto 2 Imaging System at 20X magnification (ThermoFisher Scientific). Captured images were analyzed using ImageJ analysis software. Average cross-sectional area (CSA) was quantified by tracing 150 fibers per section outlined by laminin. Myonuclei were quantified by $DAPI^{+}Pax7^{-}$ nuclei that were beneath the basal lamina. $Pax7^{+}/MyoD^{-}$ and $DAPI^{+}$ nuclei located under the basal lamina were counted as quiescent satellite cells, $Pax7^{+}/MyoD^{+}$ nuclei were identified as committed satellite cells, and $Pax7^{-}/MyoD^{+}$ nuclei were enumerated as differentiating satellite cells. Satellite cell content was expressed relative to total area analyzed. FAP cells were counted if they stained positive for PDGFRα, were associated with DAPI, and localized at the interstitial space of muscle tissue[34]. FAP content was expressed relative to total area analyzed. NF-κB activity was enumerated if nuclei ($DAPI^{+}$) positive for p-NF-κB overlapped with myonuclei or interstitial nuclei found in the interstitium. Total p-

NF-κB nuclei content (i.e. myonuclei and interstitial nuclei) was expressed relative to total area analyzed. Myonuclear p-NF- κB content was expressed relative to the total number of moynuclei. Interstitial p-NF-κB cell content was expressed relative to the total number of interstitial myonuclei. Perilipin was quantified by measuring the intensity of the perilipin stain. The intensity of perilipin was expressed as integrated density relative to total area analyzed. Quantification of collagen was based off a previous protocol[35]. Briefly, to separate collagen (blue) from muscle fibers (red) and nuclei (black/blue), collagen was quantified by thresholding. The threshold allowed us to highlight the blue collagen fibers and just measure the integrated density of that specific area. The intensity of the thresholded area was measured and expressed as integrated density relative to total area analyzed. Investigators were blinded to group during quantification.

Statistical analysis

Two-way repeated measures ANOVA was used to analyze lean mass. For all other data, except fiber distribution, a one-factor (group) ANOVA and Tukey's post-hoc test in GraphPad Prism 5 (GraphPad Software, Inc., La Jolla, CA) were used. For fiber distribution a two-way ANOVA and Bonferroni's post-hoc test in GraphPad Prism 5 (GraphPad Software, Inc., La Jolla, CA) were used. Data were presented as mean ± SEM with $p<0.05$ considered significant.

RESULTS

High fat diet altered body weight, fat mass, and lean mass

A schematic of the study design is presented in Figure 1a. Longitudinal body weight and body fat percentage across the study are presented in our companion paper (Emmons et al., unpublished). HFD-SED and HFD-EX had a higher increase in body weight from baseline to before AOM injections, relative to the CON group ($p<0.05$, Figure 1b). HFD-SED and HFD-EX mice had significantly lower changes in body weight from before AOM injections to the end of

the study, relative to the CON group ($p<0.05$, Figure 1c). HFD-SED and HFD-EX had a higher increase in percent fat mass from baseline to before AOM injections, relative to the CON group ($p<0.05$, Figure 1d). HFD-SED and HFD-EX mice had significantly lower changes in percent fat mass from before AOM injections to the end of the study, relative to the CON group ($p<0.05$, Figure 1e). From 9 to 21 weeks of age, HFD mice had increased lean mass ($p<0.05$ vs. CON, Figure 1f). At 25 weeks of age, HFD-SED mice had increased lean mass ($p<0.05$ vs. CON, Figure 1f). At 29 weeks of age, HFD-EX mice had increased lean mass ($p<0.05$ vs. CON, Figure 1f). From 33 to 41 weeks of age, lean mass was significantly increased in both HFD-SED and HFD-EX relative to CON ($p<0.05$, Figure 1f). Lean mass was not different between HFD-SED and HFD-EX at any point during the study.

Persistent alterations in muscle morphology even after weight loss without exercise

Tibialis anterior (TA) weight was significantly greater in HFD-EX relative to CON ($p<0.05$, Figure 1g). When normalized to body weight, there were no differences in TA weight between groups (Figure 1h). There were no differences in muscle cross-sectional area (CSA), myonuclei per fibre, or myonuclear domain between groups (Figure 2a, c, and d). There was a significant increase in the proportion of medium-sized fibers (900-1199 μm^2) in the HFD-SED ($p<0.01$) and HFD-EX ($p<0.05$) groups compared to CON (Figure 2b).

Representative trichrome images of muscle fibrosis are presented in Figure 3a. HFD-SED mice had greater amounts of collagen relative to HFD-EX and CON ($p<0.05$, Figure 3b). Representative images of perilipin (marker of lipid droplet) can be found in Figure 3c. HFD-SED mice also had greater amounts perilipin relative to CON ($p<0.05$, Figure 3d). There were no differences in the amount of collagen or perilipin between CON and HFD-EX groups.

Exercise increased the number of proliferating satellite cells and fibroadipogenic progenitors (FAPs)

Representative images of satellite cells and myoblast subpopulations are presented in Figure 4a and Figure 4d. There were no differences in the total number of $Pax7^+$ cells (Figure 4b), quiescent ($Pax7^+MyoD^-$, Figure 4c) satellite cells, or differentiated ($Pax7^-MyoD^+$, Figure 4f) myoblasts per area. With exercise, there was an increase in the number of committed myoblasts ($Pax7^+MyoD^+$) per area relative to CON mice ($p<0.05$, Figure 4e). A representative image of FAPs is presented in Figure 5a. Exercise increased the number of FAPs per area in comparison to CON mice ($p<0.05$, Figure 5b).

p-NF-κB is decreased following exercise

Immunofluorescent staining of nuclear p-NF-κB (Figure 6a and b) showed that total p-NFκB (i.e. myonuclear and interstitial nuclei) was decreased in the HFD-EX group in comparison to CON and HFD-SED ($p<0.05$, Figure 6c). There were no differences in the number of p-NF-$κB^+$ myonuclei per area or relative to total myonuclei (Figure 6d and e). There was a significant decrease in interstitial p-NF-$κB^+$ nuclei in the HFD-EX group relative to CON and HFD-SED ($p<0.05$, Figure 6f). There were no differences in interstitial p-NF-$κB^+$ nuclei when expressed relative to total number of interstitial nuclei (Figure 6g).

DISCUSSION

The purpose of this study was to determine the influence of weight loss with or without exercise on muscle morphology and stem/progenitor cell populations during CRC initiation. We demonstrated that exercise training resulted in lower fibro/fatty tissue accumulation in skeletal muscle in our experimental conditions. Exercise training also increased the number of committed

myoblasts and the number of FAPs. With exercise training, there was also a decrease in total p-NF-κB$^+$ nuclei which was primarily due to a decrease in interstitial p-NF-κB$^+$ nuclei. Together, this study reports the novel finding that the addition of an exercise intervention during weight loss, but not weight loss by diet alone, may be effective for stimulating myogenesis and reducing fibrosis and adiposity in mice that were previously obese during CRC initiation.

Muscle health and morphological characteristics have yet to be described as they relate to weight loss interventions during the initiation of CRC. Both obesity and cancer are associated with muscle atrophy[36,37]. As such, one would expect to see decreases in muscle weight and CSA, especially when cancer is combined with a HFD, and when compared to an exercising group. Here, we observe no differences in TA muscle weight and CSA across all groups. However, there were increases in the proportion of fibres between 900-1199 μm^2 in the HFD-EX group. Similar findings were reported by Pincu et al. (2015), whereby a concomitant HFD and exercise protocol did not result in any changes in mean CSA, but there was an increase in the proportion of fibers between 500-1000 μm^2 [29]. Pincu and colleagues suggest that the increase in fibres of this size may be due to an increase in the relative proportion of type 1 fibers because of the endurance exercise protocol[29]. This may also be true for our study. Collectively, these results suggest that this diet and exercise protocol, during the CRC initiation in previously obese mice, did not alter relative muscle weight or CSA.

Satellite cells are indispensable during the formation of new muscle, and repair of existing muscle, following physiological and pathological stimuli[12,14,38]. Cancer and obesity are conditions that result in repeated damage to the myofiber, which initiates regeneration; however, in these conditions, muscle regeneration is impaired, ultimately contributing to muscle wasting[16,17]. The primary defect in cachexia is a reduction in myoblast commitment to the myogenic lineage due to

sustained upregulation of Pax7 induced by p-NF-kB signaling[18]. Conversely, exercise has been found to facilitate the myogenic program[38]. Although we did not observe any differences in the total number of $Pax7^+$ cells between groups, the number of committed myoblasts was significantly increased with exercise. Similarly, FAP content was significantly higher in exercise trained mice. FAPs have been reported to promote myogenic commitment of activated satellite cells[11]. Thus, reduced NF-κB signaling and increased FAP content could be responsible for the observed increase in committed myoblasts. Although the increase in committed myoblasts did not result in increased myofibre CSA, it could have resulted in increased myonuclear turnover[39]. Further, given the recently discovered role of myoblasts in regulating muscle fibrosis[40], higher numbers of committed myoblasts could have contributed to the lower fibrosis observed in exercise trained mice. We speculate that this slight exercise training-induced shift in myogenic subpopulations to increase committed myoblasts could delay the onset of key characteristics of cachexia (i.e. impaired myoblast commitment and muscle fibrosis). Future, long-term studies with severe cachexia will investigate this hypothesis.

Satellite cells and FAPs reside in a complex, dynamic niche. Inflammatory conditions within muscle can influence the fate of satellite cells and FAPs. Cachexia and obesity are characterized by chronic inflammation[6,41]. However, the regulatory effects of this chronic inflammation on satellite cell and FAP function are not well understood. In other conditions, such as aging, increases in pro-inflammatory cytokines such as TNF-α and IL-1 have been found to block myogenic differentiation, and chronic elevations in IL-6 has been found to impair satellite cell mediated regeneration[42–44]. Furthermore, p-NF-κB, a transcription factor involved in inflammatory signaling, has been linked to muscle wasting in cancer cachexia[18]. Exercise, on the other hand, is well established as having anti-inflammatory effects[45]. The mechanisms through

which exercise exerts its beneficial effects on muscle remodeling also have yet to be elucidated. In a mouse model of colon cancer, treadmill running was able to prevent the progression of cachexia[46]. This may be due to reduced inflammation[45]. We observed a decrease in total p-NF-κB in the HFD-EX group which aligns with the current literature. We also measured interstitial p-NF-κB because one study found that interstitial NF-κB, that also stained positive for pericytes, impaired differentiation of co-cultured myoblasts[23]. When p-NF-κB activation was decreased, Hyldahl (2011) found that primary pericytes had increased myogenic potential[23]. We observed a decrease in interstitial p-NF-κB in the HFD-EX group, suggesting that exercise provides favourable conditions for myogenesis. As a result, this suggests that the progressive treadmill exercise protocol, following a HFD, was sufficient to reduce p-NF-κB activity in the HFD-EX mice and may explain why we observed an increase in committed myoblasts in the HFD-EX group.

These findings suggest that a HFD, followed by a weight loss intervention with exercise, prevents an increase in fibrotic and fatty tissue and is associated with an increase in committed myoblasts and FAPs during CRC initiation. The results also demonstrate lower NF-kB activation in HFD-EX. Together, the data suggests that exercise training, added to a weight loss intervention, could improve muscle health and maintain conditions that promote myogenic commitment of satellite cells during CRC initiation. Since there is currently no effective therapy for cachexia, identifying the effects of host factors on early indicators of muscle remodeling could lead to the development of therapeutic strategies that delay or prevent the onset of cachexia. As such, these findings provide the rationale to further examine the inclusion of exercise alongside diet as a means of protecting muscle health during weight loss interventions in persons at elevated risk of developing CRC.

ACKNOWLEDGEMENTS

RE, MD, HC, and YXP contributed to study design and direction. RE, DHS, GX, SR, and DD performed experiments. SR, and DD contributed to analysis. SR, and MD wrote the manuscript with contributions from all authors. All authors approved final submission.

Sources of funding: University of Illinois Urbana-Champaign Research Board, and American College of Sports Medicine.

DISCLOSURES

The authors have no financial conflicts of interest to disclose.

REFERENCES

1. Canadian Cancer Society's Advisory Committee on Cancer Statistics. *Canadian Cancer Statistics 2017*. Toronto, ON: Canadian Cancer Society; 2017. Available at: cancer.ca/Canadian-Cancer-Statistics-2017-EN.pdf. Accessed April 1, 2018.

2. Ma, Y. *et al.* Obesity and risk of colorectal cancer: a systematic review of prospective studies. *PloS One* **8,** e53916 (2013).

3. American Cancer Society. Cancer Facts & Figures 2018. Atlanta: American Cancer Society; 2018.

4. Hector, A. J. & Phillips, S. M. Protein Recommendations for Weight Loss in Elite Athletes: A Focus on Body Composition and Performance. *Int. J. Sport Nutr. Exerc. Metab.* **28,** 170–177 (2018).

5. Kumar, N. B. *et al.* Cancer cachexia: traditional therapies and novel molecular mechanism-based approaches to treatment. *Curr. Treat. Options Oncol.* **11,** 107–117 (2010).

6. Argilés, J. M., Busquets, S., Stemmler, B. & López-Soriano, F. J. Cancer cachexia: understanding the molecular basis. *Nat. Rev. Cancer* **14,** 754–762 (2014).

7. Snow, M. H. Myogenic cell formation in regenerating rat skeletal muscle injured by mincing. II. An autoradiographic study. *Anat. Rec.* **188,** 201–217 (1977).

8. Seale, P. *et al.* Pax7 is required for the specification of myogenic satellite cells. *Cell* **102,** 777–786 (2000).

9. Davis, R. L., Weintraub, H. & Lassar, A. B. Expression of a single transfected cDNA converts fibroblasts to myoblasts. *Cell* **51,** 987–1000 (1987).

10. Yin, H., Price, F. & Rudnicki, M. A. Satellite Cells and the Muscle Stem Cell Niche. *Physiol. Rev.* **93,** 23–67 (2013).

11. Joe, A. W. B. *et al.* Muscle injury activates resident fibro/adipogenic progenitors that facilitate myogenesis. *Nat. Cell Biol.* **12,** 153–163 (2010).

12. Lepper, C., Partridge, T. A. & Fan, C.-M. An absolute requirement for Pax7-positive satellite cells in acute injury-induced skeletal muscle regeneration. *Dev. Camb. Engl.* **138,** 3639–3646 (2011).

13. Murphy, M. M., Lawson, J. A., Mathew, S. J., Hutcheson, D. A. & Kardon, G. Satellite cells, connective tissue fibroblasts and their interactions are crucial for muscle regeneration. *Dev. Camb. Engl.* **138,** 3625–3637 (2011).

14. Sambasivan, R. *et al.* Pax7-expressing satellite cells are indispensable for adult skeletal muscle regeneration. *Dev. Camb. Engl.* **138,** 3647–3656 (2011).

15. Roberts, E. W. *et al.* Depletion of stromal cells expressing fibroblast activation protein-α from skeletal muscle and bone marrow results in cachexia and anemia. *J. Exp. Med.* **210,** 1137–1151 (2013).

16. Talbert, E. E. & Guttridge, D. C. Impaired regeneration: A role for the muscle microenvironment in cancer cachexia. *Semin. Cell Dev. Biol.* **54,** 82–91 (2016).

17. Akhmedov, D. & Berdeaux, R. The effects of obesity on skeletal muscle regeneration. *Front. Physiol.* **4,** 371 (2013).

18. He, W. A. *et al.* NF-κB-mediated Pax7 dysregulation in the muscle microenvironment promotes cancer cachexia. *J. Clin. Invest.* **123,** 4821–4835 (2013).

19. Talbert, E. E., Metzger, G. A., He, W. A. & Guttridge, D. C. Modeling human cancer cachexia in colon 26 tumor-bearing adult mice. *J. Cachexia Sarcopenia Muscle* **5,** 321–328 (2014).

20. Sciorati, C. *et al.* Necdin is expressed in cachectic skeletal muscle to protect fibers from tumor-induced wasting. *J. Cell Sci.* **122,** 1119–1125 (2009).

21. Penna, F. *et al.* Combined approach to counteract experimental cancer cachexia: eicosapentaenoic acid and training exercise. *J. Cachexia Sarcopenia Muscle* **2,** 95–104 (2011).

22. Rybinski, B., Franco-Barraza, J. & Cukierman, E. The wound healing, chronic fibrosis, and cancer progression triad. *Physiol. Genomics* **46,** 223–244 (2014).

23. Hyldahl, R., Schwartz, L. & M Clarkson, P. NF-KB activity functions in primary pericytes in a cell- and non-cell-autonomous manner to affect myotube formation. *Muscle Nerve* **47,** (2013).

24. Woo, M. *et al.* Early Life Nutrition Modulates Muscle Stem Cell Number: Implications for Muscle Mass and Repair. *Stem Cells Dev.* **20,** 1763–1769 (2011).

25. Chen, S.-E., Jin, B. & Li, Y.-P. TNF-α regulates myogenesis and muscle regeneration by activating p38 MAPK. *Am. J. Physiol. Cell Physiol.* **292,** C1660–C1671 (2007).

26. Farup, J. *et al.* Pericyte response to contraction mode-specific resistance exercise training in human skeletal muscle. *J. Appl. Physiol.* **119,** 1053–1063 (2015).

27. Valero, M. C., Huntsman, H. D., Liu, J., Zou, K. & Boppart, M. D. Eccentric Exercise Facilitates Mesenchymal Stem Cell Appearance in Skeletal Muscle. *PLOS ONE* **7,** e29760 (2012).

28. Huntsman, H. D. *et al.* Mesenchymal stem cells contribute to vascular growth in skeletal muscle in response to eccentric exercise. *Am. J. Physiol.-Heart Circ. Physiol.* **304,** H72–H81 (2012).

29. Pincu, Y., Linden, M. A., Zou, K., Baynard, T. & Boppart, M. D. The effects of high fat diet and moderate exercise on TGFβ1 and collagen deposition in mouse skeletal muscle. *Cytokine* **73,** 23–29 (2015).

30. Deuster, P. A., Morrison, S. D. & Ahrens, R. A. Endurance exercise modifies cachexia of tumor growth in rats. *Med. Sci. Sports Exerc.* **17,** 385–392 (1985).

31. Pincu, Y. *et al.* Diet-induced obesity regulates adipose-resident stromal cell quantity and extracellular matrix gene expression. *Stem Cell Res.* **17,** 181–190 (2016).

32. Kelly, S. A., Nehrenberg, D. L., Hua, K., Garland, T. & Pomp, D. Exercise, weight loss, and changes in body composition in mice: phenotypic relationships and genetic architecture. *Physiol. Genomics* **43,** 199–212 (2011).

33. Masson, P. Trichrome stainings and their preliminary techniques. **12,** 75 (1929).

34. Uezumi, A., Fukada, S., Yamamoto, N., Takeda, S. & Tsuchida, K. Mesenchymal progenitors distinct from satellite cells contribute to ectopic fat cell formation in skeletal muscle. *Nat. Cell Biol.* **12,** 143–152 (2010).

35. Chen, Y., Yu, Q. & Xu, C.-B. A convenient method for quantifying collagen fibers in atherosclerotic lesions by ImageJ software. *Int J Clin Exp Med.* **10**, 14904-14910 (2017).

36. Acharyya, S. *et al.* Dystrophin glycoprotein complex dysfunction: A regulatory link between muscular dystrophy and cancer cachexia. *Cancer Cell* **8,** 421–432 (2005).

37. Hu, Z. *et al.* PTEN inhibition improves muscle regeneration in mice fed a high-fat diet. *Diabetes* **59,** 1312–1320 (2010).

38. Parise, G., McKinnell, I. W. & Rudnicki, M. A. Muscle satellite cell and atypical myogenic progenitor response following exercise. *Muscle Nerve* **37,** 611–619 (2008).

39. Burd, N. A. & De Lisio, M. Skeletal Muscle Remodeling: Interconnections Between Stem Cells and Protein Turnover. *Exerc. Sport Sci. Rev.* **45,** 187–191 (2017).

40. Fry, C. S., Kirby, T. J., Kosmac, K., McCarthy, J. J. & Peterson, C. A. Myogenic Progenitor Cells Control Extracellular Matrix Production by Fibroblasts during Skeletal Muscle Hypertrophy. *Cell Stem Cell* **20,** 56–69 (2017).

41. Sinha, I., Sakthivel, D. & Varon, D. E. Systemic Regulators of Skeletal Muscle Regeneration in Obesity. *Front. Endocrinol.* **8,** (2017).

42. McKay, B. R. *et al.* Elevated SOCS3 and altered IL-6 signaling is associated with age-related human muscle stem cell dysfunction. *Am. J. Physiol. Cell Physiol.* **304,** C717-728 (2013).

43. Degens, H. Age-related skeletal muscle dysfunction: causes and mechanisms. *J. Musculoskelet. Neuronal Interact.* **7,** 246–252 (2007).

44. Trendelenburg, A. U., Meyer, A., Jacobi, C., Feige, J. N. & Glass, D. J. TAK-1/p38/nNFκB signaling inhibits myoblast differentiation by increasing levels of Activin A. *Skelet. Muscle* **2,** 3 (2012).

45. Bowen, T. S., Schuler, G. & Adams, V. Skeletal muscle wasting in cachexia and sarcopenia: molecular pathophysiology and impact of exercise training. *J. Cachexia Sarcopenia Muscle* **6,** 197–207 (2015).

46. Gould, D. W., Lahart, I., Carmichael, A. R., Koutedakis, Y. & Metsios, G. S. Cancer cachexia prevention via physical exercise: molecular mechanisms. *J. Cachexia Sarcopenia Muscle* **4,** 111–124 (2013).

FIGURE LEGENDS

Fig. 1 Changes in body weight, fat mass, lean mass and tibialis anterior (TA) weight (a) An overview of the study protocol. (b) Body weight increased in HFD-SED and HFD-EX from baseline to before AOM injections. *p<0.05 vs. CON. (c) Body weight decreased in HFD-SED and HFD-EX from before AOM injections to the end of the study. *p<0.05 vs. CON. (d) Percent fat mass increased in HFD-SED and HFD-EX from baseline to before AOM injections. *p<0.05 vs. CON. (e) Percent fat mass decreased in HFD-SED and HFD-EX from before AOM injections to the end of the study. *p<0.05 vs. CON. (f) Lean mass increased in the HFD-SED and HFD-EX groups. *p<0.05 HFD-SED vs. CON, +p<0.05 HFD-EX vs. CON (g) TA weight increased in the HFD-EX group. +p<0.05 HFD-EX vs. CON (h) TA weight was not different across groups when normalized to body weight. n=12 CON and HFD-EX, n=13 HFD-SED; data are presented as mean ± SEM.

Fig. 2 Exercise increases the proportion of medium sized fibers (a) Muscle fibre cross-sectional area. (b) Distribution of myofiber cross-sectional area from TA muscles of each experimental group. (c) The number of myonuclei per fibre. (d) Myonuclear domain. +p<0.05 HFD-EX vs. CON, **p<0.05 HFD-EX vs. HFD-SED; n=11 CON, n=12 HFD-SED and HFD-EX; data are presented as mean ± SEM.

Fig. 3 Muscle fibrosis and adiposity are elevated in previously obese mice without exercise (a) Representative images of muscle fibrosis; n=10 CON and HFD-EX, n=11 HFD-SED. (b) An increase in muscle fibrosis was demonstrated in the HFD-SED group (expressed as integrated density/area). (c) Representative images of perilipin; n=10 CON and HFD-SED, n=8 HFD-EX (d) Adiposity was increased in the HFD-SED group (expressed as integrated density/area). *p<0.05 HFD-SED vs. CON, **p<0.05 HFD-EX vs. HFD-SED; data are presented as mean ± SEM.

Fig. 4 Exercise is associated with an increase in committed myoblasts (a) Representative image of a quiescent satellite cell ($Pax7^{+}MyoD^{-}$). (b) The total number of satellite cells. (c) The number of quiescent satellite cells ($Pax7^{+}MyoD^{-}$). (d) Representative image of a committed myoblasts ($Pax7^{+}MyoD^{+}$). (e) Exercise increased the number of committed myoblasts ($Pax7^{+}MyoD^{+}$). (f) The number of differentiated myoblasts ($Pax7^{-}MyoD^{+}$). +$p<0.05$ HFD-EX vs. CON; n=11 CON, n=10 HFD-SED, n=12 HFD-EX; data are presented as mean ± SEM.

Fig. 5 FAPs are increased in the HFD-EX group relative to CON (a) Representative image of a FAP. (b) Exercise increased the number of FAP ($PDGFR\alpha^{+}$). +$p<0.05$ HFD-EX vs. CON; n=12 CON, n=10 HFD-SED, n=11 HFD-EX; data are presented as mean ± SEM.

Fig. 6 Exercise is associated with decreased nuclear p-NF-kB (a) Representative image of p-NF-κB^{+} myonuclei. (b) Representative image of p-NF-κB^{+} non-myonuclei (c) The total number of p-NF-κB^{+} cells per area decreased in the HFD-EX group. (d) The number of p-NF-κB^{+} myonuclei expressed per area. (e) The number of p-NF-κB^{+} myonuclei expressed relative to the total number of myonuclei. (f) The number of p-NF-κB^{+} non-myonuclei expressed per area decreased in the HFD-EX group. (g) The number of p-NF-κB^{+} non-myonuclei expressed relative to the total number of non-myonuclei. +$p<0.05$ HFD-EX vs. CON, **HFD-EX vs. HFD-SED; n=11 CON and HFD-SED, n=12 HFD-EX; data are presented as mean ± SEM.

FIGURES

Figure 1.

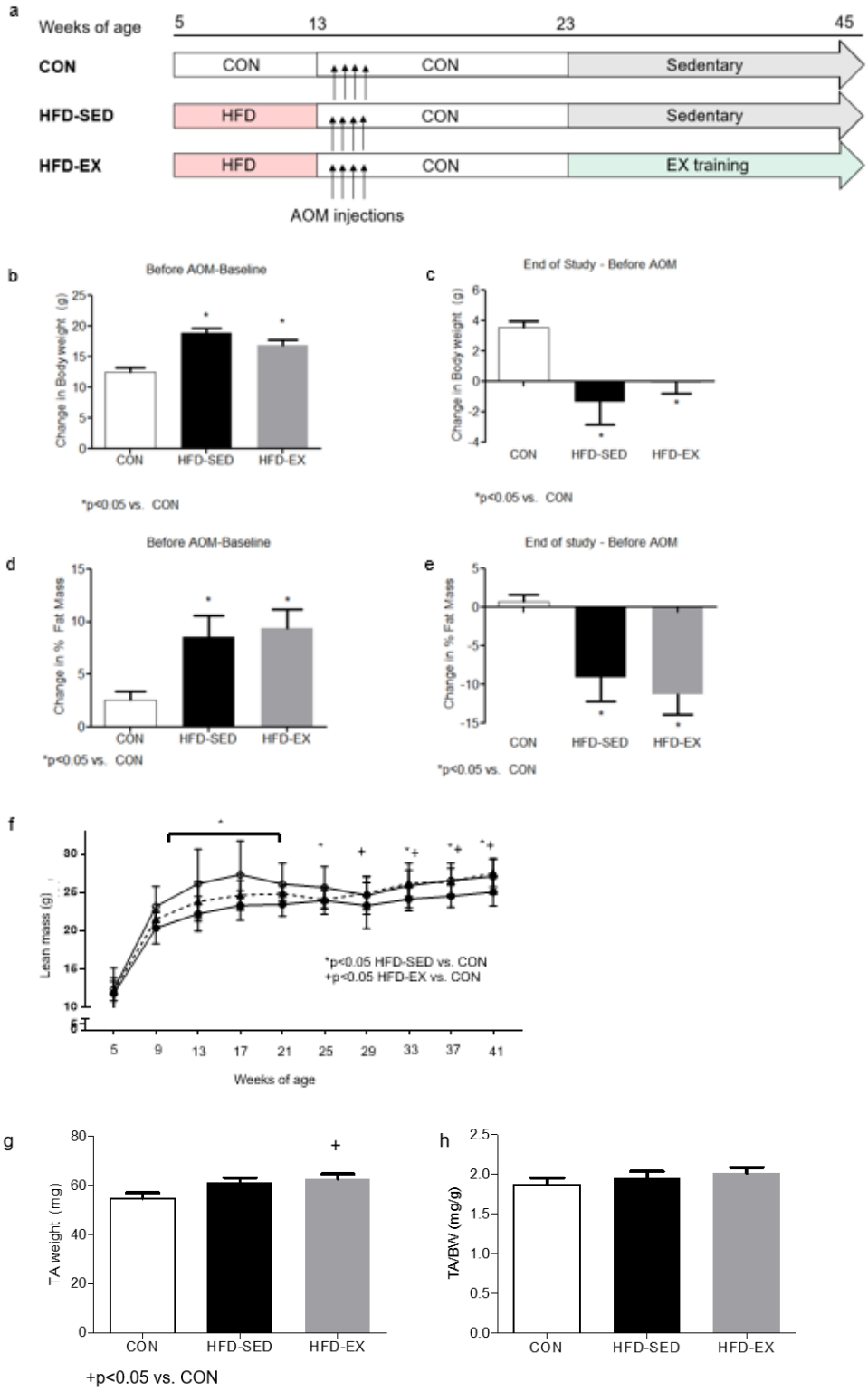

Figure 2.

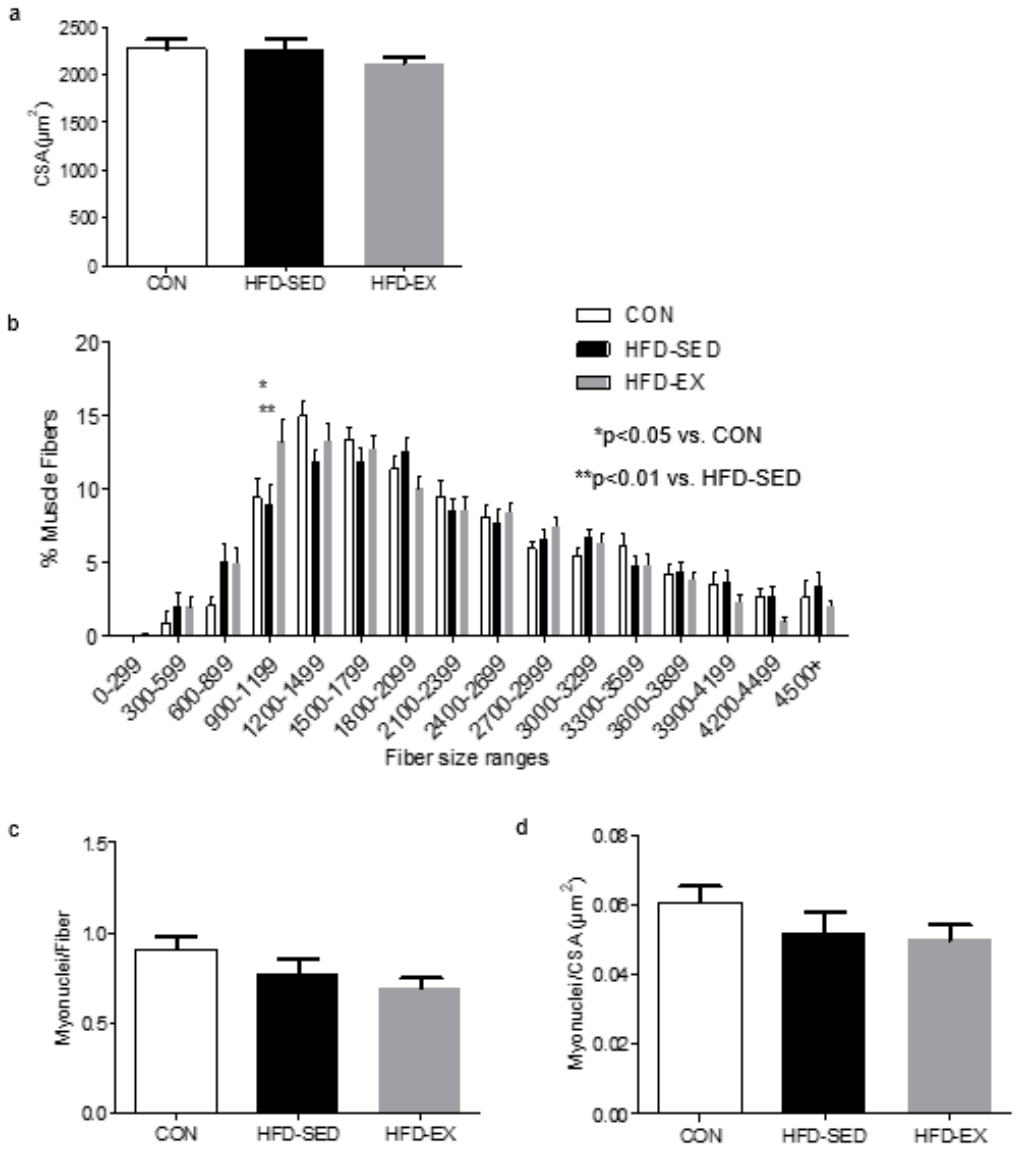
a
CSA(μm²)
2500
2000
1500
1000
500
0
CON
HFD-SED
HFD-EX
b
CON
HFD-SED
HFD-EX
*p<0.05 vs. CON
**p<0.01 vs. HFD-SED
% Muscle Fibers
20
15
10
5
0
*
**
0-299
300-599
600-899
900-1199
1200-1499
1500-1799
1800-2099
2100-2399
2400-2699
2700-2999
3000-3299
3300-3599
3600-3899
3900-4199
4200-4499
4500+
Fiber size ranges
c
Myonuclei/Fiber
1.5
1.0
0.5
0.0
CON
HFD-SED
HFD-EX
d
Myonuclei/CSA (μm²)
0.08
0.06
0.04
0.02
0.00
CON
HFD-SED
HFD-EX

Figure 3.

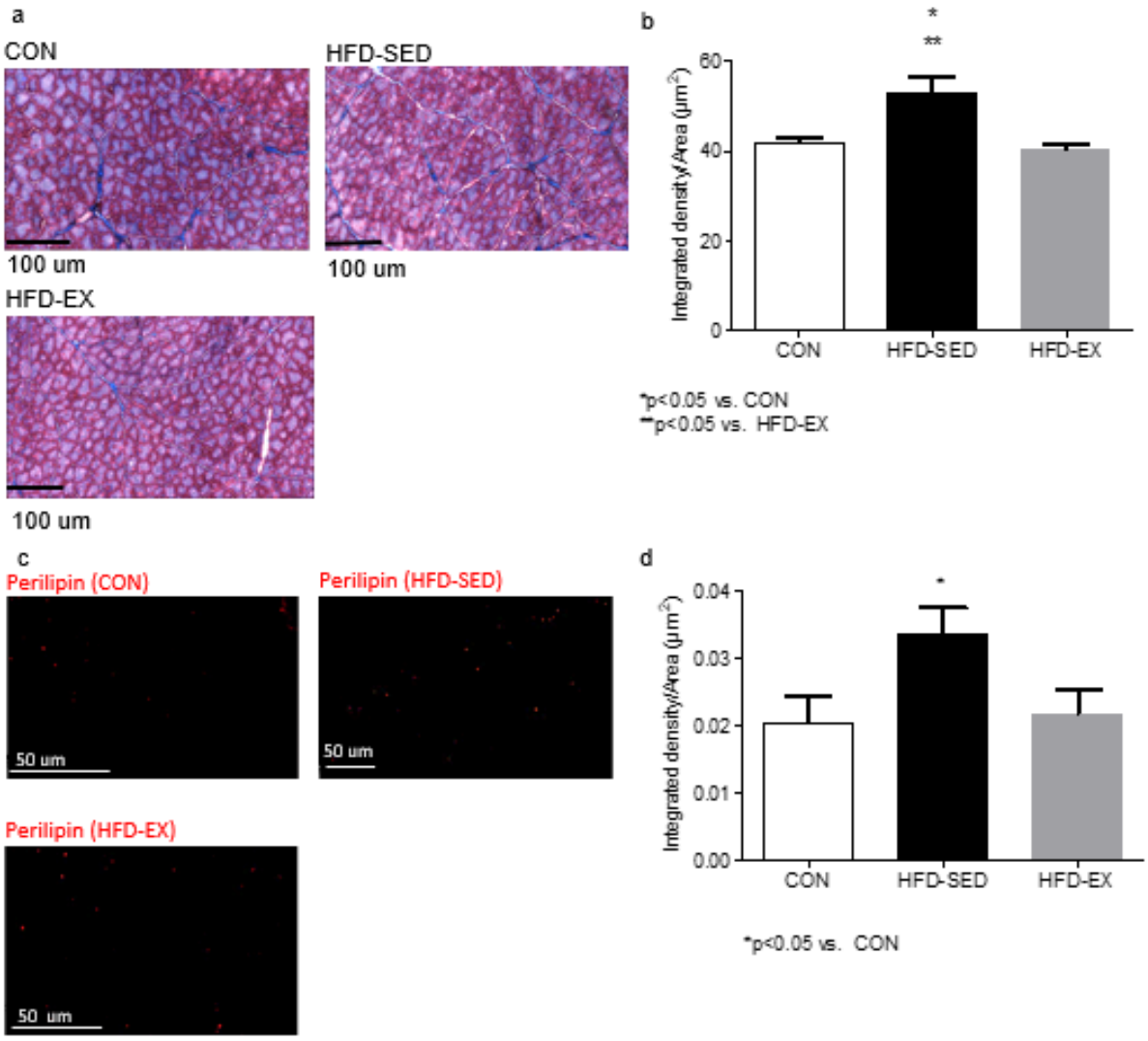
a
CON
HFD-SED
100 um
100 um
HFD-EX
100 um
b
Integrated density/Area (µm²)
60
40
20
0
CON
HFD-SED
HFD-EX
*
**
*p<0.05 vs. CON
**p<0.05 vs. HFD-EX
c
Perilipin (CON)
Perilipin (HFD-SED)
50 um
50 um
Perilipin (HFD-EX)
50 um
d
Integrated density/Area (µm²)
0.04
0.03
0.02
0.01
0.00
CON
HFD-SED
HFD-EX
*
*p<0.05 vs. CON

Figure 4.

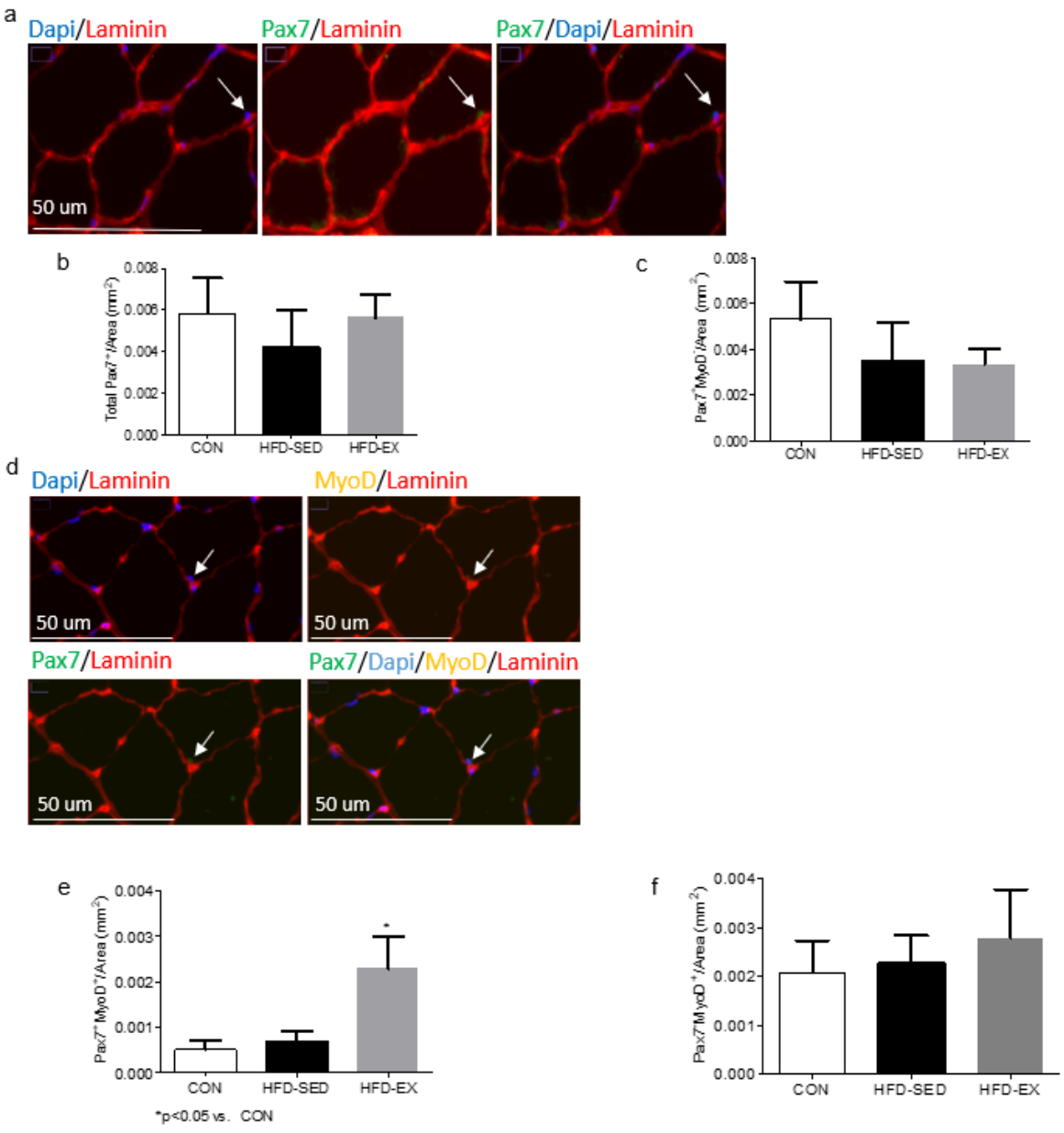
a
Dapi/Laminin
Pax7/Laminin
Pax7/Dapi/Laminin
50 um
b
Total Pax7+/Area (mm2)
0.008
0.006
0.004
0.002
0.000
CON
HFD-SED
HFD-EX
c
Pax7+MyoD-/Area (mm2)
0.008
0.006
0.004
0.002
0.000
CON
HFD-SED
HFD-EX
d
Dapi/Laminin
MyoD/Laminin
Pax7/Laminin
Pax7/Dapi/MyoD/Laminin
50 um
e
Pax7+ MyoD+/Area (mm2)
0.004
0.003
0.002
0.001
0.000
*
CON
HFD-SED
HFD-EX
*p<0.05 vs. CON
f
Pax7+MyoD+/Area (mm2)
0.004
0.003
0.002
0.001
0.000
CON
HFD-SED
HFD-EX

Figure 5.

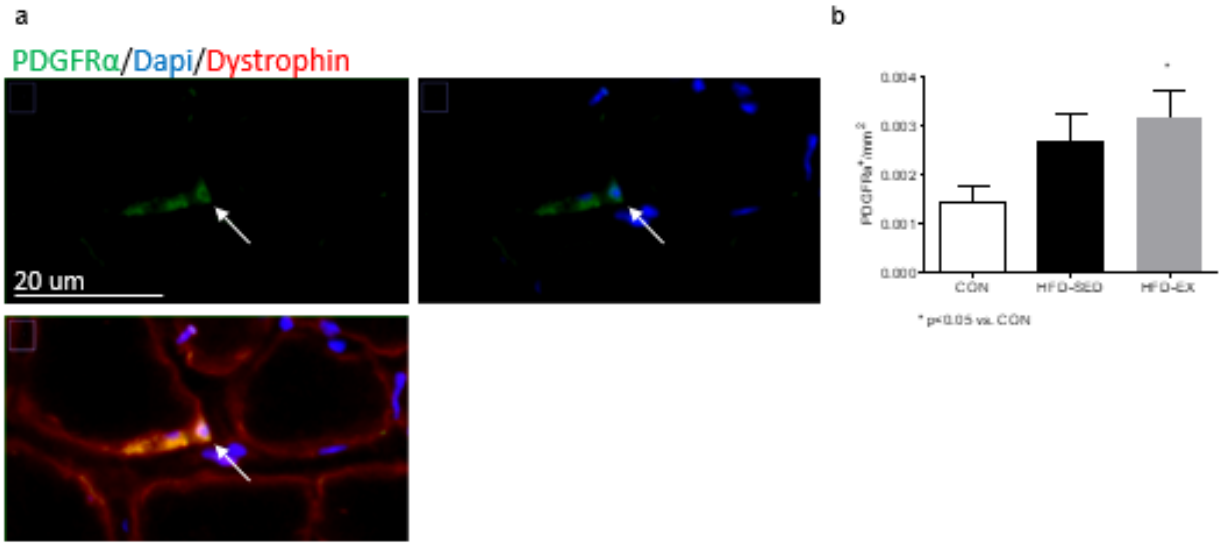
a
PDGFRα/Dapi/Dystrophin
20 um
b
0.004
0.003
0.002
0.001
0.000
CON
HFD-SED
HFD-EX
* p<0.05 vs. CON

Figure 6.

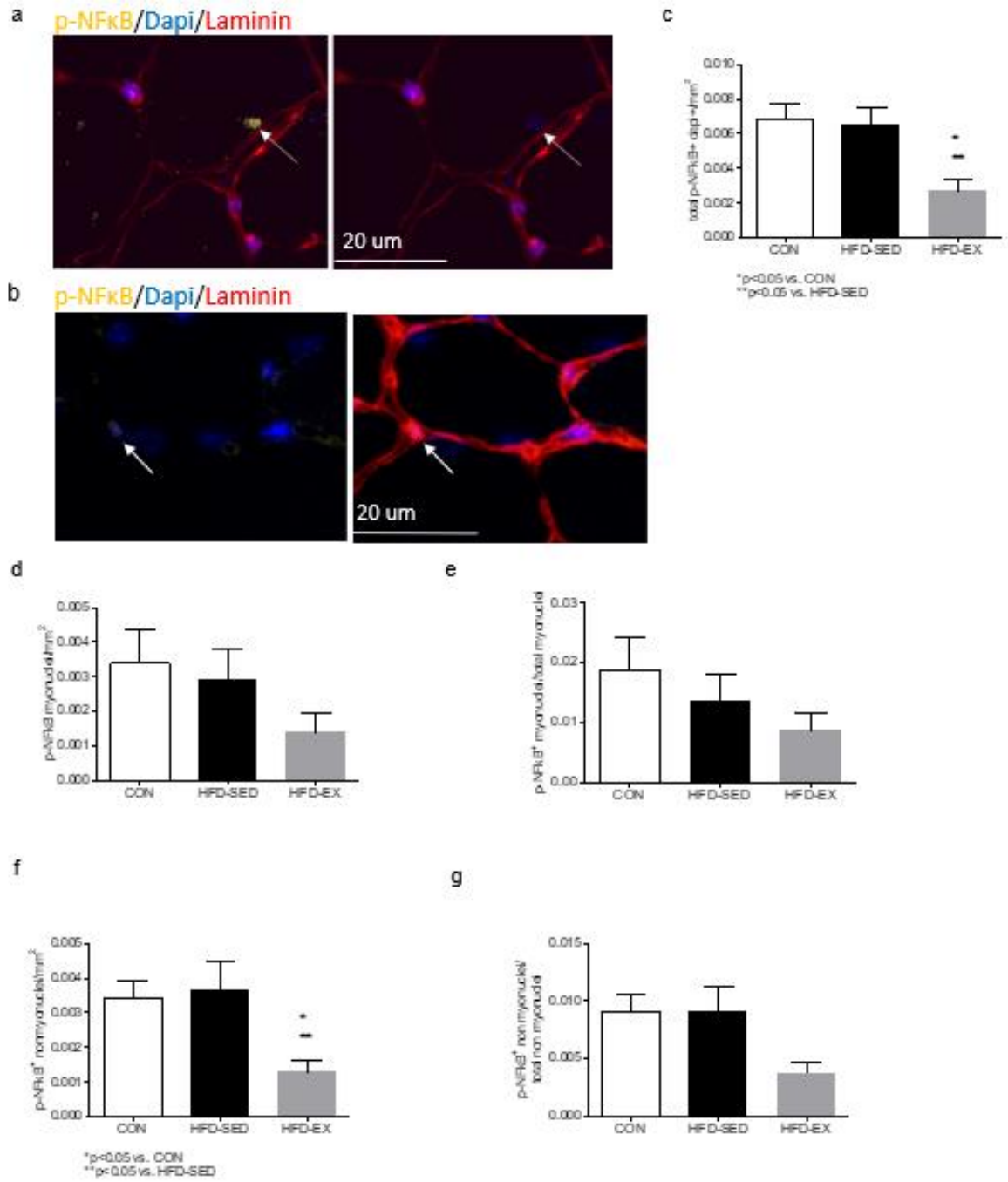
a
p-NFκB/Dapi/Laminin
20 um
b
p-NFκB/Dapi/Laminin
20 um
c
CON
HFD-SED
HFD-EX
*p<0.05 vs. CON
**p<0.05 vs. HFD-SED
d
CON
HFD-SED
HFD-EX
e
CON
HFD-SED
HFD-EX
f
CON
HFD-SED
HFD-EX
*p<0.05 vs. CON
**p<0.05 vs. HFD-SED
g
CON
HFD-SED
HFD-EX

PART III

Global Discussion

Cachexia, characterized by severe muscle atrophy and fibro/fatty tissue accumulation is common in many patients with advanced cancers (Rybinski, Franco-Barraza, & Cukierman, 2014). Currently, there is no effective therapy for cachexia, thus the best approach is prevention (Argilés et al., 2014). Identifying lifestyle factors, and early cellular indicators that might predict or contribute to cachexia would provide novel preventative strategies. Obesity is associated with an increased risk of cancer, particularly CRC (Ma et al., 2013). As such, persons at high-risk of developing CRC are often recommended to undergo a weight loss program to reduce their CRC risk (American Cancer Society, 2018). Early life obesity followed by weight loss can reduce skeletal muscle mass; however, exercise may preserve muscle mass during weight loss (Bowen et al., 2015; Santanasto et al., 2011). The overall aim of the present study was to determine the effects of weight loss with or without exercise training on markers of muscle morphology and remodeling in a model of CRC. We used the chemical carcinogen, AOM, to induce CRC because it allowed us to study non-hereditary factors (i.e. obesity, weight loss, and exercise), and allowed us to induce the disease at any time. In addition, the preneoplastic lesions developed due to the administration of AOM mimic those in human CRC and create a similar inflammatory environment that is also present in human CRC development (Suzui, Morioka, & Yoshimi, 2013). A HFD consisting of 45% kcal from fat was used because this is typical of a Western diet. We chose to study treadmill exercise because it is highly reproducible and has been found to facilitate myogenesis (Shefer, Rauner, Stuelsatz, Benayahu, & Yablonka-Reuveni, 2013). The exercise was progressive to ensure continued adaptation to the protocol. We studied the TA muscle because it is primarily comprised of type II fibers, which are more susceptible to atrophy (Acharyya et al., 2005). Lastly, we chose

to study this model in C57BL/6J mice primarily because they are susceptible to diet-induced obesity, which allowed us to induce obesity, then study weight loss interventions in obese mice (Wang & Liao, 2012).

To assess muscle morphology, muscle health, and stem/progenitor populations we selected several markers. Individual muscle fibers are surrounded by the endomysium, also known as the basal lamina (Yin et al., 2013). As such, to measure CSA, we used laminin, a well-known marker of the basal lamina (Tamaki, Akatsuka, Yoshimura, Roy, & Edgerton, 2002). Staining the basal lamina was also necessary to determine the location of satellite cells, which are found between the basal lamina and the sarcolemma (Mauro, 1961). Satellite cells can be identified using immunofluorescence by staining for satellite cell-specific transcription factors. It is widely accepted that quiescent satellite cells express Pax7 but not MyoD (Cornelison & Wold, 1997). As satellite cells become committed to the myogenic lineage, they also express MyoD (Cooper et al., 1999; Cornelison & Wold, 1997; Füchtbauer & Westphal, 1992). To initiate differentiation, Pax7 expression is downregulated (Chen et al., 2010). FAPs are non-myogenic progenitors also found in muscle and are commonly identified in muscle by staining for PDGFRα (Uezumi et al., 2014; Uezumi et al., 2011). Fibrosis is an accumulation of ECM proteins, with collagen being the primary component (Uezumi et al., 2011). As such, using Masson's trichrome stain to identify collagen was a justified way of measuring fibrosis in our model. To measure adiposity, an increased level of fat in muscle, we stained for perilipin. Perilipins are found on the surface of adipocytes and lipid droplets, and as such, reflect the level of adiposity in muscle (Kalinkovich & Livshits, 2017). Together, the markers we chose to analyze muscle morphology, health and stem/progenitor populations are well-established methods of detection.

To more directly measure the inflammatory conditions within muscle, a cytokine array analysis was performed (Appendix A). There were no biologically relevant differences (defined as ≥1.5 fold change) in cytokines. The largest change observed was a 1.37-fold increase in IL-12p70 in the HFD-EX group relative to CON (Appendix A). IL-12p70 is the biologically active form of IL-12 (Watford, Moriguchi, Morinobu, & O'Shea, 2003). It is widely known as a major immunomodulatory cytokine (Suzuki, 2018). There are very few studies that examine IL-12p70 as it relates to myogenesis. One study found that an over expression of IL-12 facilitates differentiation of C2C12 myoblasts in a co-culture system (Romanazzo, Forte, Morishima, & Taniguchi, 2015). It may be that IL-12p70 may have had a similar effect in our exercising group. In addition, we speculate that there may not have been many changes in cytokine level in muscle because if present in high concentrations, they would have been released into the circulation. As such, it is more likely that cytokines would be observed in greater quantity in the blood. A sufficient quantity of blood to perform these analyses was not available. Despite this, the data suggests that diet to induce weight loss, followed by exercise, may facilitate myogenesis by reducing levels of IL-12p70. However, the strength of this data is limited because we only measured cytokine levels in one pooled sample per group using a semi-quantitative analysis.

The primary limitation of this study was only analyzing the TA muscle. The TA muscle was a justified choice because atrophying fibers are selectively type II (Acharyya et al., 2005). However, a more complete picture of muscle health could have been attained by analyzing different muscles, particularly those comprised of a mix of type I and type II fibers. Another limitation of this study is that we had to pool samples to run the cytokine array, and the array is only semi-quantitative. This prevented us from being able to statistically analyze differences between groups. Further, blood samples were not available to conduct similar analyses in plasma

or serum. Lastly, the mice only developed pre-neoplastic lesions. This is a limitation that warrants careful interpretation of the findings, given that as the tumor grows, so does the inflammatory environment, which could have a substantial impact on the myogenic and progenitor cell populations examined. In our companion study, HFD-SED mice had a significantly higher number of preneoplastic lesions than both other groups. As such, the differences we observed in skeletal muscle could have been due to higher preneoplastic burden. Future studies will compare groups with similarly advanced tumors.

These findings extend our knowledge about weight loss interventions during CRC with respect to muscle health. Additional research is necessary to determine the specific mechanisms associated with the benefits of endurance exercise on muscle quality during CRC. Future studies may also be beneficial to determine whether these findings can be extended to those with late stage cancer, rather than early stage cancer, as this is when muscle loss becomes most pronounced. In conclusion, we demonstrated that diet, followed by exercise, can maintain muscle health during the progression of CRC.

PART IV

Statement of contribution

RE, MD, HC, and YXP contributed to study design and direction. RE, DHS, GX, SR, and DD performed experiments. SR, and DD contributed to analysis. SR and MD wrote the manuscript with contributions from all authors.

PART V

References

Acharyya, S., Butchbach, M. E. R., Sahenk, Z., Wang, H., Saji, M., Carathers, M., … Guttridge, D. C. (2005). Dystrophin glycoprotein complex dysfunction: A regulatory link between muscular dystrophy and cancer cachexia. *Cancer Cell*, *8*(5), 421–432. https://doi.org/10.1016/j.ccr.2005.10.004

Akhmedov, D., & Berdeaux, R. (2013). The effects of obesity on skeletal muscle regeneration. *Frontiers in Physiology*, *4*, 371. https://doi.org/10.3389/fphys.2013.00371

American Cancer Society. Cancer Facts & Figures 2018. Atlanta: American Cancer Society; 2018.

Argilés, J. M., Busquets, S., Stemmler, B., & López-Soriano, F. J. (2014). Cancer cachexia: understanding the molecular basis. *Nature Reviews Cancer*, *14*(11), 754–762. https://doi.org/10.1038/nrc3829

Boppart, M. D., De Lisio, M., Zou, K., & Huntsman, H. D. (2013). Defining a role for non-satellite stem cells in the regulation of muscle repair following exercise. *Frontiers in Physiology*, *4*. https://doi.org/10.3389/fphys.2013.00310

Bossola, M., Marzetti, E., Rosa, F., & Pacelli, F. (2016). Skeletal muscle regeneration in cancer cachexia. *Clinical and Experimental Pharmacology and Physiology*, *43*(5), 522–527. https://doi.org/10.1111/1440-1681.12559

Bowen, T. S., Schuler, G., & Adams, V. (2015). Skeletal muscle wasting in cachexia and

sarcopenia: molecular pathophysiology and impact of exercise training. *Journal of Cachexia, Sarcopenia and Muscle*, *6*(3), 197–207. https://doi.org/10.1002/jcsm.12043

Canadian Cancer Society's Advisory Committee on Cancer Statistics. *Canadian Cancer Statistics 2017*. Toronto, ON: Canadian Cancer Society; 2017. Available at: cancer.ca/Canadian-Cancer-Statistics-2017-EN.pdf (accessed April 1, 2018).

Chen, J.-F., Tao, Y., Li, J., Deng, Z., Yan, Z., Xiao, X., & Wang, D.-Z. (2010). microRNA-1 and microRNA-206 regulate skeletal muscle satellite cell proliferation and differentiation by repressing Pax7. *The Journal of Cell Biology*, *190*(5), 867–879. https://doi.org/10.1083/jcb.200911036

Collins, C. A., & Partridge, T. A. (2005). Self-Renewal of the Adult Skeletal Muscle Satellite Cell. *Cell Cycle*, *4*(10), 1338–1341. https://doi.org/10.4161/cc.4.10.2114

Cooper, R. N., Tajbakhsh, S., Mouly, V., Cossu, G., Buckingham, M., & Butler-Browne, G. S. (1999). In vivo satellite cell activation via Myf5 and MyoD in regenerating mouse skeletal muscle. *Journal of Cell Science*, *112 (Pt 17)*, 2895–2901.

Cornelison, D. D. W., & Wold, B. J. (1997). Single-Cell Analysis of Regulatory Gene Expression in Quiescent and Activated Mouse Skeletal Muscle Satellite Cells. *Developmental Biology*, *191*(2), 270–283. https://doi.org/10.1006/dbio.1997.8721

Courneya, K. S., & Friedenreich, C. M. (1997). Relationship Between Exercise Pattern Across the

Cancer Experience and Current Quality of Life in Colorectal Cancer Survivors. *The Journal of Alternative and Complementary Medicine*, *3*(3), 215–226. https://doi.org/10.1089/acm.1997.3.215

Davis, R. L., Weintraub, H., & Lassar, A. B. (1987). Expression of a single transfected cDNA converts fibroblasts to myoblasts. *Cell*, *51*(6), 987–1000. https://doi.org/10.1016/0092-8674(87)90585-X

Donohoe, C. L., Ryan, A. M., & Reynolds, J. V. (2011). Cancer Cachexia: Mechanisms and Clinical Implications. *Gastroenterology Research and Practice*, *2011*. https://doi.org/10.1155/2011/601434

D'Souza, D. M., Trajcevski, K. E., Al-Sajee, D., Wang, D. C., Thomas, M., Anderson, J. E., & Hawke, T. J. (2015). Diet-induced obesity impairs muscle satellite cell activation and muscle repair through alterations in hepatocyte growth factor signaling. *Physiological Reports*, *3*(8). https://doi.org/10.14814/phy2.12506

Farup, J., De Lisio, M., Rahbek, S. K., Bjerre, J., Vendelbo, M. H., Boppart, M. D., & Vissing, K. (2015). Pericyte response to contraction mode-specific resistance exercise training in human skeletal muscle. *Journal of Applied Physiology*, *119*(10), 1053–1063. https://doi.org/10.1152/japplphysiol.01108.2014

Fu, X., Zhu, M., Zhang, S., Foretz, M., Viollet, B., & Du, M. (2016). Obesity Impairs Skeletal Muscle Regeneration Through Inhibition of AMPK. *Diabetes*, *65*(1), 188–200. https://doi.org/10.2337/db15-0647

Füchtbauer, E. M., & Westphal, H. (1992). MyoD and myogenin are coexpressed in regenerating skeletal muscle of the mouse. *Developmental Dynamics: An Official Publication of the American Association of Anatomists*, *193*(1), 34–39. https://doi.org/10.1002/aja.1001930106

Gould, D. W., Lahart, I., Carmichael, A. R., Koutedakis, Y., & Metsios, G. S. (2013). Cancer cachexia prevention via physical exercise: molecular mechanisms. *Journal of Cachexia, Sarcopenia and Muscle*, *4*(2), 111–124. https://doi.org/10.1007/s13539-012-0096-0

He, W. A., Berardi, E., Cardillo, V. M., Acharyya, S., Aulino, P., Thomas-Ahner, J., … Guttridge, D. C. (2013). NF-κB-mediated Pax7 dysregulation in the muscle microenvironment promotes cancer cachexia. *The Journal of Clinical Investigation*, *123*(11), 4821–4835. https://doi.org/10.1172/JCI68523

Hu, Z., Wang, H., Lee, I. H., Modi, S., Wang, X., Du, J., & Mitch, W. E. (2010). PTEN inhibition improves muscle regeneration in mice fed a high-fat diet. *Diabetes*, *59*(6), 1312–1320. https://doi.org/10.2337/db09-1155

Huntsman, H. D., Zachwieja, N., Zou, K., Ripchik, P., Valero, M. C., De Lisio, M., & Boppart, M. D. (2012). Mesenchymal stem cells contribute to vascular growth in skeletal muscle in response to eccentric exercise. *American Journal of Physiology-Heart and Circulatory Physiology*, *304*(1), H72–H81. https://doi.org/10.1152/ajpheart.00541.2012

Irwin, M. L., Crumley, D., McTiernan, A., Bernstein, L., Baumgartner, R., Gilliland, F. D., …

Ballard-Barbash, R. (2003). Physical activity levels before and after a diagnosis of breast cancer: The Health, Eating, Activity, and Lifestyle (HEAL) Study. *Cancer*, *97*(7), 1746–1757. https://doi.org/10.1002/cncr.11227

Joe, A. W. B., Yi, L., Natarajan, A., Grand, F. L., So, L., Wang, J., … Rossi, F. M. V. (2010). Muscle injury activates resident fibro/adipogenic progenitors that facilitate myogenesis. *Nature Cell Biology*, *12*(2), 153–163. https://doi.org/10.1038/ncb2015

Kalinkovich, A., & Livshits, G. (2017). Sarcopenic obesity or obese sarcopenia: A cross talk between age-associated adipose tissue and skeletal muscle inflammation as a main mechanism of the pathogenesis. *Ageing Research Reviews*, *35*, 200–221. https://doi.org/10.1016/j.arr.2016.09.008

Kumar, N. B., Kazi, A., Smith, T., Crocker, T., Yu, D., Reich, R. R., … Bepler, G. (2010). Cancer cachexia: traditional therapies and novel molecular mechanism-based approaches to treatment. *Current Treatment Options in Oncology*, *11*(3–4), 107–117. https://doi.org/10.1007/s11864-010-0127-z

Lepper, C., Partridge, T. A., & Fan, C.-M. (2011). An absolute requirement for Pax7-positive satellite cells in acute injury-induced skeletal muscle regeneration. *Development (Cambridge, England)*, *138*(17), 3639–3646. https://doi.org/10.1242/dev.067595

Ma, Y., Yang, Y., Wang, F., Zhang, P., Shi, C., Zou, Y., & Qin, H. (2013). Obesity and risk of colorectal cancer: a systematic review of prospective studies. *PloS One*, *8*(1), e53916. https://doi.org/10.1371/journal.pone.0053916

Martin, L., Birdsell, L., Macdonald, N., Reiman, T., Clandinin, M. T., McCargar, L. J., … Baracos, V. E. (2013). Cancer cachexia in the age of obesity: skeletal muscle depletion is a powerful prognostic factor, independent of body mass index. *Journal of Clinical Oncology: Official Journal of the American Society of Clinical Oncology*, *31*(12), 1539–1547. https://doi.org/10.1200/JCO.2012.45.2722

Mauro, A. (1961). Satellite cell of skeletal muscle fibers. *The Journal of Biophysical and Biochemical Cytology*, *9*, 493–495.

Mehl, K. A., Davis, J. M., Berger, F. G., & Carson, J. A. (2005). Myofiber degeneration/regeneration is induced in the cachectic *Apc* $^{Min/+}$ mouse. *Journal of Applied Physiology*, *99*(6), 2379–2387. https://doi.org/10.1152/japplphysiol.00778.2005

Murphy, M. M., Lawson, J. A., Mathew, S. J., Hutcheson, D. A., & Kardon, G. (2011). Satellite cells, connective tissue fibroblasts and their interactions are crucial for muscle regeneration. *Development (Cambridge, England)*, *138*(17), 3625–3637. https://doi.org/10.1242/dev.064162

Olguin, H. C., Yang, Z., Tapscott, S. J., & Olwin, B. B. (2007). Reciprocal inhibition between Pax7 and muscle regulatory factors modulates myogenic cell fate determination. *The Journal of Cell Biology*, *177*(5), 769–779. https://doi.org/10.1083/jcb.200608122

Penna, F., Busquets, S., Pin, F., Toledo, M., Baccino, F. M., López-Soriano, F. J., … Argilés, J.

M. (2011). Combined approach to counteract experimental cancer cachexia: eicosapentaenoic acid and training exercise. *Journal of Cachexia, Sarcopenia and Muscle*, *2*(2), 95–104. https://doi.org/10.1007/s13539-011-0028-4

Pincu, Y., Huntsman, H. D., Zou, K., De Lisio, M., Mahmassani, Z. S., Munroe, M. R., … Boppart, M. D. (2016). Diet-induced obesity regulates adipose-resident stromal cell quantity and extracellular matrix gene expression. *Stem Cell Research*, *17*(1), 181–190. https://doi.org/10.1016/j.scr.2016.07.002

Pincu, Y., Linden, M. A., Zou, K., Baynard, T., & Boppart, M. D. (2015). The effects of high fat diet and moderate exercise on TGFβ1 and collagen deposition in mouse skeletal muscle. *Cytokine*, *73*(1), 23–29. https://doi.org/10.1016/j.cyto.2015.01.013

Potthoff, M. J., Olson, E. N., & Bassel-Duby, R. (2007). Skeletal muscle remodeling. *Current Opinion in Rheumatology*, *19*(6), 542. https://doi.org/10.1097/BOR.0b013e3282efb761

Roberts, E. W., Deonarine, A., Jones, J. O., Denton, A. E., Feig, C., Lyons, S. K., … Fearon, D.T. (2013). Depletion of stromal cells expressing fibroblast activation protein-α from skeletal muscle and bone marrow results in cachexia and anemia. *The Journal of Experimental Medicine*, *210*(6), 1137–1151. https://doi.org/10.1084/jem.20122344

Romanazzo, S., Forte, G., Morishima, K., & Taniguchi, A. (2015). IL-12 involvement in myogenic differentiation of C2C12 in vitro. *Biomaterials Science*, *3*(3), 469–479. https://doi.org/10.1039/C4BM00315B

Rybinski, B., Franco-Barraza, J., & Cukierman, E. (2014). The wound healing, chronic fibrosis,

and cancer progression triad. *Physiological Genomics*, *46*(7), 223–244. https://doi.org/10.1152/physiolgenomics.00158.2013

Sambasivan, R., Yao, R., Kissenpfennig, A., Van Wittenberghe, L., Paldi, A., Gayraud-Morel, B., … Galy, A. (2011). Pax7-expressing satellite cells are indispensable for adult skeletal muscle regeneration. *Development (Cambridge, England)*, *138*(17), 3647–3656. https://doi.org/10.1242/dev.067587

Santanasto, A. J., Glynn, N. W., Newman, M. A., Taylor, C. A., Brooks, M. M., Goodpaster, B. H., & Newman, A. B. (2011). Impact of Weight Loss on Physical Function with Changes in Strength, Muscle Mass, and Muscle Fat Infiltration in Overweight to Moderately Obese Older Adults: A Randomized Clinical Trial [Research article]. https://doi.org/10.1155/2011/516576

Sciorati, C., Touvier, T., Buono, R., Pessina, P., François, S., Perrotta, C., … Brunelli, S. (2009). Necdin is expressed in cachectic skeletal muscle to protect fibers from tumor-induced wasting. *Journal of Cell Science*, *122*(Pt 8), 1119–1125. https://doi.org/10.1242/jcs.041665

Seale, P., Sabourin, L. A., Girgis-Gabardo, A., Mansouri, A., Gruss, P., & Rudnicki, M. A. (2000). Pax7 is required for the specification of myogenic satellite cells. *Cell*, *102*(6), 777–786.

Shefer, G., Rauner, G., Stuelsatz, P., Benayahu, D., & Yablonka-Reuveni, Z. (2013). Moderate-intensity treadmill running promotes expansion of the satellite cell pool in young and old mice. *The FEBS Journal*, *280*(17), 4063–4073. https://doi.org/10.1111/febs.12228

Snow, M. H. (1977). Myogenic cell formation in regenerating rat skeletal muscle injured by mincing. II. An autoradiographic study. *The Anatomical Record*, *188*(2), 201–217. https://doi.org/10.1002/ar.1091880206

Suzui, M., Morioka, T., & Yoshimi, N. (2013). Colon Preneoplastic Lesions in Animal Models. *Journal of Toxicologic Pathology*, *26*(4), 335–341. https://doi.org/10.1293/tox.2013-0028

Suzuki, K. (2018). Cytokine Response to Exercise and Its Modulation. *Antioxidants*, *7*(1). https://doi.org/10.3390/antiox7010017

Talbert, E. E., & Guttridge, D. C. (2016). Impaired regeneration: A role for the muscle microenvironment in cancer cachexia. *Seminars in Cell & Developmental Biology*, *54*, 82–91. https://doi.org/10.1016/j.semcdb.2015.09.009

Talbert, E. E., Metzger, G. A., He, W. A., & Guttridge, D. C. (2014). Modeling human cancer cachexia in colon 26 tumor-bearing adult mice. *Journal of Cachexia, Sarcopenia and Muscle*, *5*(4), 321–328. https://doi.org/10.1007/s13539-014-0141-2

Tamaki, T., Akatsuka, A., Yoshimura, S., Roy, R. R., & Edgerton, V. R. (2002). New Fiber Formation in the Interstitial Spaces of Rat Skeletal Muscle During Postnatal Growth. *Journal of Histochemistry & Cytochemistry*, *50*(8), 1097–1111. https://doi.org/10.1177/002215540205000812

Tatsumi, R., Hattori, A., Ikeuchi, Y., Anderson, J. E., & Allen, R. E. (2002). Release of Hepatocyte

Growth Factor from Mechanically Stretched Skeletal Muscle Satellite Cells and Role of pH and Nitric Oxide. *Molecular Biology of the Cell*, *13*(8), 2909–2918. https://doi.org/10.1091/mbc.E02-01-0062

Toth, M. J., Callahan, D. M., Miller, M. S., Tourville, T. W., Hackett, S. B., Couch, M. E., & Dittus, K. (2016). Skeletal muscle fiber size and fiber type distribution in human cancer: Effects of weight loss and relationship to physical function. *Clinical Nutrition*, *35*(6), 1359–1365. https://doi.org/10.1016/j.clnu.2016.02.016

Uezumi, A, Fukada, S., Yamamoto, N., Ikemoto-Uezumi, M., Nakatani, M., Morita, M., … Tsuchida, K. (2014). Identification and characterization of PDGFRα+ mesenchymal progenitors in human skeletal muscle. *Cell Death & Disease*, *5*(4), e1186. https://doi.org/10.1038/cddis.2014.161

Uezumi, Akiyoshi, Ito, T., Morikawa, D., Shimizu, N., Yoneda, T., Segawa, M., … Fukada, S. (2011). Fibrosis and adipogenesis originate from a common mesenchymal progenitor in skeletal muscle. *J Cell Sci*, *124*(21), 3654–3664. https://doi.org/10.1242/jcs.086629

Valero, M. C., Huntsman, H. D., Liu, J., Zou, K., & Boppart, M. D. (2012). Eccentric Exercise Facilitates Mesenchymal Stem Cell Appearance in Skeletal Muscle. *PLOS ONE*, *7*(1), e29760. https://doi.org/10.1371/journal.pone.0029760

Wang, C.-Y., & Liao, J. K. (2012). A Mouse Model of Diet-Induced Obesity and Insulin Resistance. *Methods in Molecular Biology (Clifton, N.J.)*, *821*, 421–433. https://doi.org/10.1007/978-1-61779-430-8_27

Watford, W. T., Moriguchi, M., Morinobu, A., & O'Shea, J. J. (2003). The biology of IL-12: coordinating innate and adaptive immune responses. *Cytokine & Growth Factor Reviews*, *14*(5), 361–368. https://doi.org/10.1016/S1359-6101(03)00043-1

Woo, M., Isganaitis, E., Cerletti, M., Fitzpatrick, C., Wagers, A. J., Jimenez-Chillaron, J., & Patti, M. E. (2011). Early Life Nutrition Modulates Muscle Stem Cell Number: Implications for Muscle Mass and Repair. *Stem Cells and Development*, *20*(10), 1763–1769. https://doi.org/10.1089/scd.2010.0349

Yin, H., Price, F., & Rudnicki, M. A. (2013). Satellite Cells and the Muscle Stem Cell Niche. *Physiological Reviews*, *93*(1), 23–67. https://doi.org/10.1152/physrev.00043.2011

Zou, K., Huntsman, H. D., Carmen Valero, M., Adams, J., Skelton, J., De Lisio, M., … Boppart, M. D. (2015). Mesenchymal stem cells augment the adaptive response to eccentric exercise. *Medicine and Science in Sports and Exercise*, *47*(2), 315–325. https://doi.org/10.1249/MSS.0000000000000405

Appendix

Appendix A – Cytokine data

Cytokine array analysis

Optimal cutting temperature compound was removed from three TA muscles from each group, and were pooled and homogenized in 400 uL of RIPA buffer containing protease inhibitors. Fischer Scientific's bead homogenizer was used, and samples were homogenized for 2 rounds of 60 seconds. Then, samples were centrifuged at 10,000 RCF at 4℃ for 15 minutes. Supernatants were removed and frozen at -80℃. A DC assay was used to determine protein concentrations. The pooled supernatants were analyzed using the C-Series Mouse Inflammation Antibody Array C1 (Ray Bio) following the manufacturers protocol. 400 ug of protein was loaded to each array. To visualize the assays, images were captured using a ChemiDoc Imaging System (Bio-Rad). Images were analyzed using ImageJ. Briefly, integrated densities of each target were measured. The average integrated densities for each target were divided by the average of the control targets to determine a fold difference.

Cytokine Array Analysis Results

No biologically relevant differences were detected in any of the cytokines analyzed.

Cytokine Array Analysis Figure

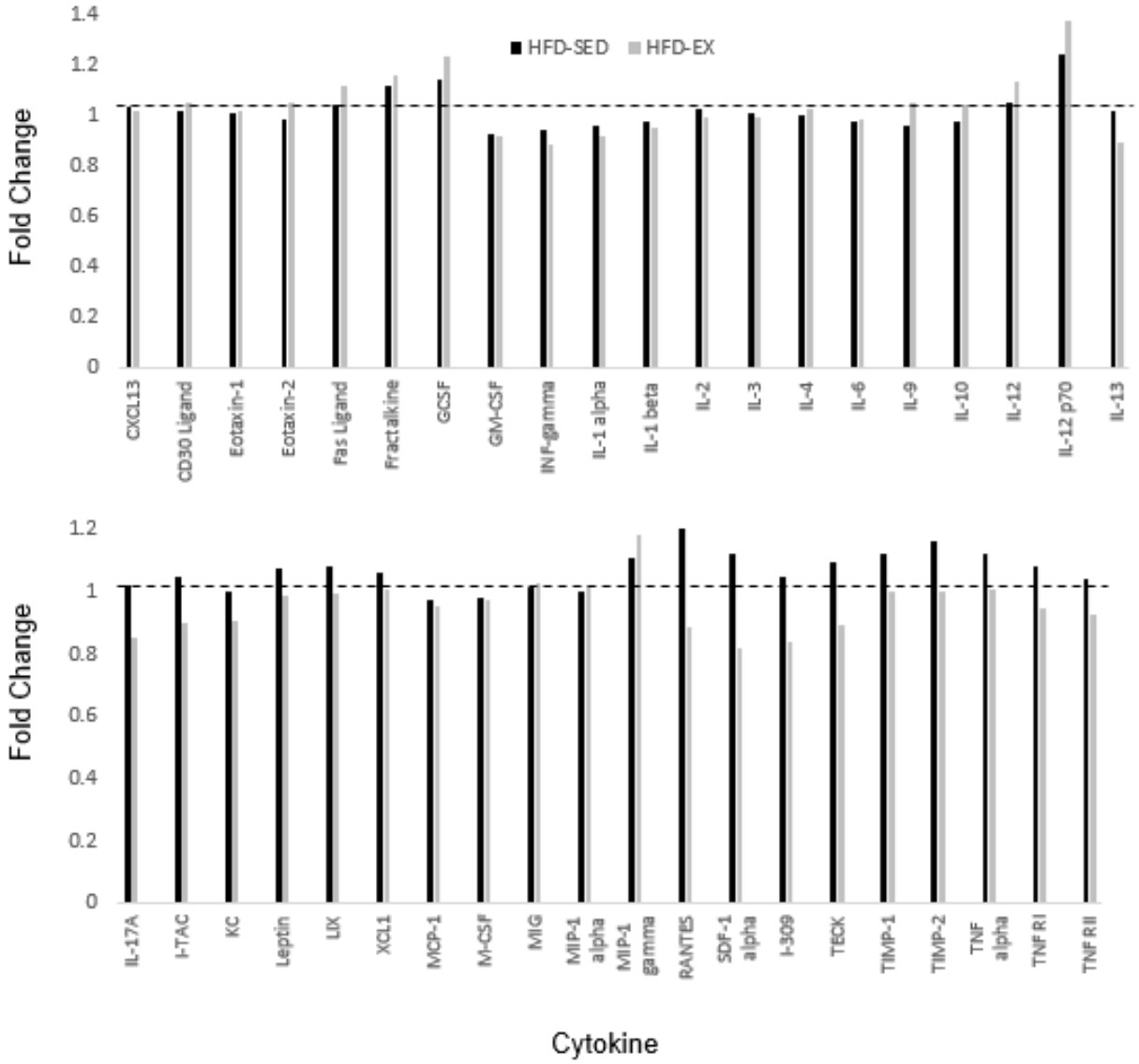

Appendix B - Protocols Used in Thesis

Pax7/MyoD/Laminin Stain

1. Allow sections to thaw and dry
2. Wash 1 x PBS, 2x3 min
3. Fix 2% PFA, 7 min @RT
4. Wash 1xPBS, 2x2 min
5. 0.1% triton, 10 min @ RT
6. Wash 1xPBS, 2x2 min
7. MOM block (2 drops IgG + 2.5 mL PBS), 1 hour at RT
8. Wash 1 x PBS, 2x2 min
9. Diluent (600 uL protein + 7.5 mL PBS), 5 min at RT
10. 1°Ab Pax7 [neat] O/N @ 4 degrees C
11. Wash 1 x PBS, 3x5 min
12. 2°Ab Ab AF488 (anti-mouse) 1:300 in 5% GS, 1 hour at RT
13. Wash 1x PBS, 3x5 min
14. Block 5% GS + 1% BSA + 0.1% triton x-100
15. 1°Ab cocktail. MyoD (rabbit) 1:100 in block, laminin (rat) 1:200 in block. O/N @ 4 degrees C
16. Wash 1x PBS, 3 x 5 min
17. Secondary cocktail, AF594 (anti-rabbit) 1:300, AF647 (anti-rat) 1:300, in 5% GS, 1 hour at RT
18. Wash 1x PBS, 2x2 min
19. Dapi 5 min

20. Wash 1 x PBS, 3 x 5 min
21. Coverslip

Perilipin Stain

1. Allow sections to thaw and dry
2. Wash 1 x PBS, 2x3 min
3. Fix 2% PFA, 7 min @ RT
4. Wash 1x PBS, 2x2 min
5. 0.1% triton x-100, 10 min @ RT
6. Wash 1 x PBS, 2 x 3 min
7. Block 5% GS + 1% BSA + 0.1% triton x-100, 1 hour @ RT
8. 1°Ab Perilipin (rabbit) 1:100 in block O/N @ 4 degrees C
9. Wash 1 x PBS, 3 x 2 min
10. 2°Ab AF594 (anti-rabbit) 1:300 in block, 1 hour at RT
11. Wash 1 x PBS, 3x3 min
12. Block (same as step 7), 1 hour @ RT
13. 1°Ab laminin (rat) 1:200 (anti rat 1.5 hours at RT)
14. Wash 3x3 min, 1 x PBS
15. 2°Ab AF647 (anti-rat) 1:300 in block, 1 hour at RT
16. Wash 3 x 2 min 1 xPBS
17. Dapi 5 min at RT (1:10 000)
18. Wash 3 x 2 min, 1 x PBS
19. Coverslip

PDGFRalpha/Dystrophin Stain

1. Allow sections to thaw and dry
2. Wash 1XPBS - 2x3 mins
3. Fix with 2% PFA for 7 mins at RT
4. Wash with 1XPBS – 2x2 mins
5. 0.1% Triton X-100 – 10 mins RT
6. Wash 2x2 min 1xPBS
7. MOM Block (2 drops 1gG + 2.5ml PBS) – 1 hr RT
8. Wash 2x2 mins 1xPBS
9. MOM Diluent (600ul protein +7.5ml PBS) – 5 min RT
10. Primary – Dystrophin (anti-mouse, Sigma) – 1 :200 (in DAKO) – O/N at 4C
11. Wash 3x3 min 1xPBS
12. Secondary – Alexa Fluora 594 (anti-mouse) 1:300 in 1xPBS 1 hr RT
    a. *KEEP IN DARK FROM THIS POINT ONWARDS*
    b. Wash 3x3 min 1xPBS
13. Block – DAKO (for PDGFRa) -1 hr RT
14. Primary – PDGFRa (anti-goat) - 1:500 (in DAKO) - O/N 4C
15. Wash 3x3min 1XPBS
16. Secondary – Alexa Fluora 488 (anti-goat) 1:300 in DAKO – 1 hr RT
17. Wash 3x3 min 1xPBS
18. DAPI – 5 min RT
19. Wash 2x2 min 1xPBS
20. Fluromont and Coverslip

p-NF-κB Stain

1. Allow sections to thaw and dry
2. Wash 1 x PBS, 2x3 min
3. Fix 2% PFA, 7 min @ RT
4. Wash 1x PBS, 2x2 min
5. 0.1% triton x-100, 10 min @ RT
6. Wash 1 x PBS, 2 x 3 min
7. Block 5% GS + 1% BSA + 0.1% triton x-100, 1 hour @ RT
8. 1°Ab p-NF-κB (rabbit) 1:200 in block O/N @ 4 degrees C
9. Wash 1 x PBS, 3 x 2 min
10. 2°Ab AF594 (anti-rabbit) 1:300 in block, 1 hour at RT
11. Wash 1 x PBS, 3x3 min
12. Block (same as step 7), 1 hour @ RT
13. 1°Ab laminin (rat) 1:200 (anti rat 1.5 hours at RT)
14. Wash 3x3 min, 1 x PBS
15. 2°Ab AF647 (anti-rat) 1:300 in block, 1 hour at RT
16. Wash 3 x 2 min 1 xPBS
17. Dapi 5 min at RT (1:10 000)
18. Wash 3 x 2 min, 1 x PBS
19. Coverslip

Scanning Muscle Sections – EVOS FL2 Microscope (Created by Donna D'Souza)

Before using the Microscope:

- Ensure you are properly trained to use the microscope and software

- Use labagenda.com to sign up for a time slot
- Ensure the required light channels are available/have been installed in the microscope. If you are unsure how to switch light cubes, please contact someone in the Burelle Lab.

Turning on the Microscope:

- Turn on all equipment (fluorescent bulb, microscope, and computer)
- Open Auto 2 program on computer, program will calibrate automatically
- Place slide in slide holder stage

Identify Section and Adjust Image

- Select the proper vessel. Ensure that the orientation is correct (i.e. facing up)
- Set objective to 20x (default), if using a higher objective, ensure proper use of microscope oil where needed.
- Select the appropriate channels for viewing. If viewing fluorescence, it is best to view the initial image using DAPI.

  Note: For fluorescent images, click settings next to bright and change mode to simple and camera to mono. For brightfield images, select camera as color.
- Move stage using the arrows on the computer or touch screen for fine movement. Set light on the section that you want.
- Increase the brightness of the image using the brightness range. Upon viewing a “blue” screen, adjust the focus using the course adjustment range. Note that this is done by selecting the buttons on each parameter and moving them accordingly, or selecting the button and using the mouse scroll to scroll through (slower adjustment, best used to refine these parameters).
- Autofocus may also be used, but tends to take a longer time to do adjust accordingly

- Select the other channels of interest and adjust accordingly
- Once satisfied with all channels, capture the image using the command located below these parameters

  Note: You must capture the channels before scanning the section.

Scanning Fluorescent Sections

- Select Automate tab. The following parameters will be available:
    - **Hardware**: select appropriate objective and channels to scan. Can select multiple channels at one time.
    - **Scan area**: Select the "create locations" tool. Then click at the top of the screen of an image with 4 boxes. This will allow you view the whole slide. You will be prompted to draw some sort of shape. Select the rectangle (or other desired shape of choice). The captured image will be highlighted by a box with a yellow outline on the slide. Estimate the approximate size of the section and create a rectangular box in this area. This will be the area that will be scanned. You may rename this area by clicking on the title "Rectangle 1".

      Tip: Rather than estimating the size of the section, prior to entering the automate tab, you can capture images all around the section. I.e. on the "Capture" tab, you can press capture, then click light, then continue to capture more images around the periphery of the section. These images will save. So, when you go into the automate tab, you will know how big your section is.
    - Once created, return to the 'Automate' tab. Here you will be prompted to add Scan Locations. Select the area you have created, and click 'Add Selected' to add this area to the 'Scan Locations' from the 'Available Locations' list.

Tip: by highlighting the name of the scan location, you can change it to the name of your section. This way you can keep track of what you have scanned.

- At the bottom of this section, you will be prompted to select the style of capturing the image (default will be Serpentine Horizontal for Area Acquisition, Outward Counter Clockwise for Filed Acquisition). It does not matter what you select.
- Select 'Stitching' to stitch individual images together to create a larger image. Once finished, select 'Done'.
- Select the 'Autofocus' tab. Select 'Single Channel' and 'DAPI' to have the section focused. The frequency can be adjusted based at the bottom of this parameter. Once finished, select 'Done'.
- Generally, muscle sections will not require 'Time Lapse', so there is no need to edit this parameter.
- To save the scanned section, go to 'image Save Settings'. Create a new folder on the computer with the desired name. Select the preferred parameters.

- Once all parameters have been adjusted, select 'Run' to begin scanning the section.
- Note that the average duration of scanning is approximately 5-10 minutes.
- Scanning lots of blank space (areas with no section present) will greatly increase the scan time. If faced with a very long scan period (greater than 10 minutes), stop the scan and readjust the scan area accordingly (this will save you time!).

ImageJ Guide

***NB: When ROI's are listed in ROI manager, highlight all ROI's. Then, press more and save. This will save all ROI's and you will be able to open individual ROI's again for the image and edit them if necessary!

Merging Images

1. Load photos into Image J. You can drag and drop the photos into ImageJ.
2. Press image (this should be at the very top of your screen)
3. Select Image → Colour → Merge channels
4. Once you press merge channels, a window will pop up.
5. Select the colours you want your images to appear as. I.e. DAPI as blue and laminin as red.

7. Press OK. The photo will merge and you can proceed.

How to count fibers (150 per section)

1. Set scale
    a. Click line bar
    b. Draw line over the scale
    c. Press analyze
    d. Click set scale
    e. Change the known distance to what the scale bar reads
    f. Change the units to microns
2. Set measurements
    a. Click Analyze

   b. Click set measurements.
   c. Select area and Feret's diameter
3. Use the kidney bean looking free hand selection.
4. Draw a circle around the fibers.
5. Hit "t" and it will add it to your ROI
6. Click show all and label
7. Press measure in window that opens up when you press "t" (this will show you the area and the Ferets)
8. Record the area and the Ferets in an excel document for each section

*Tip: measure all of them and then export. Be sure to select the right fiber when measuring.

*If fibers look elongated or very big avoid these.

<u>How to measure myonuclei</u>

- Laminin represents the basal lamina. This is what you circled when you were measuring cross sectional area.
- The blue dots represent nuclei. Not all nuclei will count as myonuclei.
- Myonuclei are any nuclei that are at least 50% beneath the basal lamina.
- You will need to manually count the number of nuclei for each fiber you measured. You can use the counter on ImageJ. It is the box that looks like stars.
- Also make note of centrally located nuclei (CLN). They are very rare and you may not see any.

Tip: when you zoom in on the photo, if you want to scroll around, hold down the space bar and click and drag the photo.

How to measure sub-populations of satellite cells, FAPs, and p-NF-κB

1. Open images and merge
2. Set the scale

   Analyze → Set scale
3. Set measurements

   Analyze → Set measurements → Area
4. Use the kidney bean looking free hand selection.
5. Draw circles around areas of fibers
6. Hit "t" and it will add it to your ROI
7. Click show all and label in the ROI window
8. Press measure in window that opens when you press "t" (this will show you the area)
9. Record the area in an excel document for each section
10. Count cells of interest

    Tips:

    Select Image → Adjust → Brightness and contrast, so you can alter the brightness of the image

    Select Image → Colour → Channels tool, to be able to view certain channels at a time. In this window, if you select colour, you can alter the brightness/contrast of that individual channel even with the merged image.

    Select Analyze → Tools → Grid. If you set a grid, it will make it easier to keep track of where and what sections you are counting. Alter the size of the grid to your preference.

How to measure perilipin

1. Open image of full section and trace around section. Save this as an ROI.

2. Open image just of perilipin. Open saved ROI in order to see outline of section.
3. Set scale
4. Select measurements
    a. Analyze → Measurements → Area and integrated density
5. Use the kidney bean looking free hand selection.
6. Draw circles around areas of fibers
7. Hit "t" and it will add it to your ROI
8. Click show all and label in the ROI window
9. Press measure in window that opens when you press "t" (this will show you the area and integrated density)

How to measure Trichrome

1. Analyze → Set scale
2. Image → Colour → Colour deconvolution
3. Select Masson Trichrome from the drop-down menu. Press ok.
4. Select the blue image
5. Image → Adjust → Threshold
6. Threshold image
7. Apply the threshold
8. Analyze → Set measurements. Select area, integrated density, limit to threshold.
9. Circle ROI's. Press t to add them to the ROI manager. Measure all ROI's.
10. Copy and paste measurements into excel. Ratio of integrated density/area. Take average of ratios for each sample.